Mitochondrial function in vivo evaluated by NADH fluorescence: from animal models to human studies

Avraham Mayevsky and Gennady G. Rogatsky

Am J Physiol Cell Physiol 292:615-640, 2007. First published Aug 30, 2006;
doi:10.1152/ajpcell.00249.2006

Am J Physiol Cell Physiol 292: C615–C640, 2007.
First published August 30, 2006; doi:10.1152/ajpcell.00249.2006.

Invited Review

Mitochondrial function in vivo evaluated by NADH fluorescence: from animal models to human studies

Avraham Mayevsky and Gennady G. Rogatsky

The Mina and Everard Goodman Faculty of Life Sciences and the Leslie and Susan Gonda Multidisciplinary Brain Research Center, Bar-Ilan University, Ramat-Gan, Israel

Mayevsky A, Rogatsky GG. Mitochondrial function in vivo evaluated by NADH fluorescence: from animal models to human studies. *Am J Physiol Cell Physiol* 292: C615–C640, 2007. First published August 30, 2006; doi:10.1152/ajpcell.00249.2006.—Normal mitochondrial function is a critical factor in maintaining cellular homeostasis in various organs of the body. Due to the involvement of mitochondrial dysfunction in many pathological states, the real-time in vivo monitoring of the mitochondrial metabolic state is crucially important. This type of monitoring in animal models as well as in patients provides real-time data that can help interpret experimental results or optimize patient treatment. The goals of the present review are the following: *1*) to provide an historical overview of NADH fluorescence monitoring and its physiological significance; *2*) to present the solid scientific ground underlying NADH fluorescence measurements based on published materials; *3*) to provide the reader with basic information on the methodologies used in the past and the current state of the art fluorometers; and *4*) to clarify the various factors affecting monitored signals, including artifacts. The large numbers of publications by different groups testify to the valuable information gathered in various experimental conditions. The monitoring of NADH levels in the tissue provides the most important information on the metabolic state of the mitochondria in terms of energy production and intracellular oxygen levels. Although NADH signals are not calibrated in absolute units, their trend monitoring is important for the interpretation of physiological or pathological situations. To understand tissue function better, the multiparametric approach has been developed where NADH serves as the key parameter. The development of new light sources in UV and visible spectra has led to the development of small compact units applicable in clinical conditions for better diagnosis of patients.

real-time tissue viability; tissue spectroscopy; patient monitoring

UNDERSTANDING THE MITOCHONDRIAL function has been a challenge for many investigators, including cytologists, biochemists, and physiologists, since its discovery more than 120 years ago. In addition to many books regarding the mitochondria, Ernster and Schatz (79) reviewed the history of mitochondrial structure and function studies. In the past two decades, several studies have reported mitochondrial involvement in pathological processes such as stroke (225) or cytoprotection (77). Most of the information on the mitochondrial function has been accumulated from in vitro studies. A relatively small portion of published papers dealt with the monitoring of mitochondrial function in vivo and in real time. Presently, examination of the involvement of the mitochondrial function in many pathological states, such as sepsis, requires monitoring of patients treated in intensive care units. Unfortunately, real-time monitoring of the mitochondrial function in patients has rarely been performed. The current study presents a review of this issue. To evaluate the activity of the respiratory chain in vivo, it is possible to monitor the mitochondrial NADH, FAD, or the cytochrome oxidase oxidation-reduction state. The interference of blood with the monitoring of FAD and cytochrome oxidase is much higher than with NADH (48); therefore, we invest our effort into the monitoring of the mitochondrial NADH redox state. We do not know of any publication showing clearly that Fp fluorescence could be monitored in vivo in blood-perfused organs. In our preliminary report, we showed that in specific brain areas, one can see the fluorescence of Fp but we were not sure how to validate the results. During the past 33 years, we have published >140 papers in this very significant area, including the largest number of studies using NADH redox state monitoring in patients.

Since the discovery of pyridine nucleotides by Harden and Young (94), >1,000 papers have been published on the use of NADH (Fig. 1*A*) as a marker for mitochondrial function. In 2000, Schleffler et al. (217) reviewed mitochondrial research methods over the past century. A major aspect of mitochondrial function, namely monitoring the energy state of tissues in vivo, was not discussed in that review. Therefore, the present review will summarize 50 years of research, started in 1955 by Chance and Williams (56, 57), by defining the mitochondrial metabolic state in vitro. To understand mitochondrial function in vivo and under various pathophysiological conditions, it is important to monitor the redox state of the respiratory chain in real time. The present review will discuss the monitoring principles for one of the electron carriers, namely, nicotinamide adenine dinucleotide (NADH). It is well known that mitochondrial dysfunction is involved in many diseases, such as ischemia, hypoxemia, Parkinson's disease, Alzheimer's disease, and in the apoptotic process. Therefore, the possibility of monitoring the mitochondrial NADH redox state in experimental animals and patients is of great importance.

Substrates and O_2 are supplied by the blood in microcirculation, namely, from the very small arterioles and the capillary bed. Glucose, the main energy substrate for the brain, enters the cells, and, after degradation in glycolysis processes, enters the TCA cycle. As a result, the NADH produced enters the respiratory chain in the mitochondria. More than 50% of the ATP synthesized by mitochondria in the brain is used by active transport processes via Na^+-K^+-ATPase. Their product is ADP, which, together with inorganic phosphate, enters the mitochondria and is resynthesized into ATP. This process demonstrates the close coupling between energy supply and demand.

To assess the energy demand, it is necessary to measure different organ-specific parameters. In the brain, the energy demand can be evaluated by measuring the extracellular levels of K^+ that reflect the activity of the major ATP consumer:

Address for reprint requests and other correspondence: A. Mayevsky, The Mina & Everard Goodman Faculty of Life Sciences and The Leslie and Susan Gonda Multidisciplinary Brain Research Center, Bar-Ilan Univ., Ramat-Gan 52900, Israel (e-mail: mayevsa@mail.biu.ac.il).

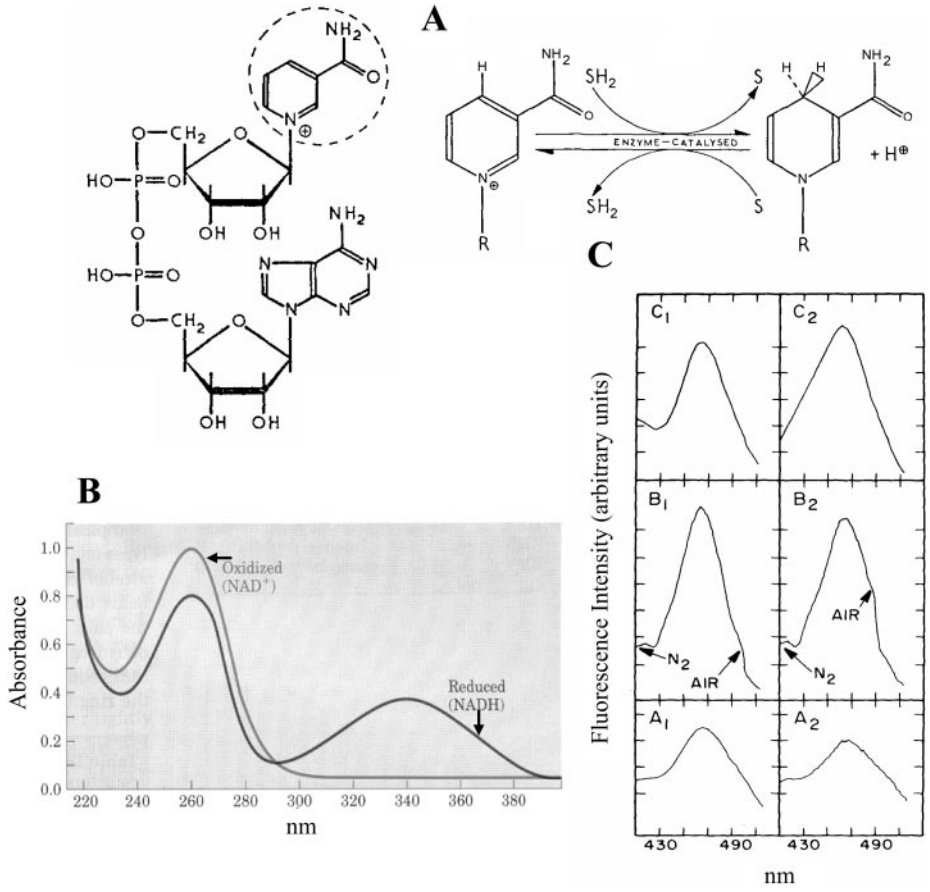

Fig. 1. *A*: molecular structure of NAD^+ and the inter-conversion of NAD^+ and NADH. *B*: difference in the absorption spectra of NAD^+ and NADH. *C*: emission spectra of brain NADH excited by 366 nm light (A1, A2, B1, B2, C1) or 324 nm laser light (C2). C1 and C2 show measurements from a dead brain, for comparison of NADH spectra using two different light sources.

Na^+-K^+-ATPase (152, 161). In the heart, most of the energy is consumed by the muscle contraction activity. On the other hand, the energy supply mechanism is the same in all tissues: oxygenated blood reaching the capillary bed releases O_2 that diffuses into the cells. Therefore, it is possible to evaluate tissue energy supply by monitoring the same four different parameters in all tissues.

The main function of the mitochondria is to convert the potential energy stored in various substrates (e.g., glucose) into ATP. The inner membrane of the mitochondria contains 5 complexes of integral membrane proteins, including NADH dehydrogenase (complex 1). Three of those proteins are involved in the respiratory chain activity. The main function of the respiratory chain is to gradually transfer electrons from NADH and $FADH_2$ (originating from the TCA cycle) to O_2. With the addition of protons (H^+), H_2O is generated in complex 4. NADH (Fig. 1*A*, *right side*) is a substrate or a coenzyme for the enzymatic activity of dehydrogenases that form part of the respiratory chain and reside in the inner membrane of the mitochondria. Further details on the biochemical properties of NADH can be found in various publications (55).

SPECTROSCOPIC MONITORING OF NADH: AN HISTORICAL OVERVIEW

The discovery of the optical properties of reduced nicotinamide adenine dinucleotide (NADH; previously known as diphosphopyridine nucleotide or pyridine nucleotide) has led to a very intensive research since the early 1950s. The reduced form of this molecule, NADH, absorbs light at 320–380 nm (Fig. 1*B*) and emits fluorescent light at the 420–480 nm range (Fig. 1*C*).

Because the oxidized form NAD^+ does not absorb light in this range, it was possible to evaluate the redox state of the mitochondria by monitoring the UV absorbance (see *Monitoring UV absorbance by NADH*) or blue fluorescence of NADH (see *Monitoring NADH fluorescence*).

Undoubtedly, the pioneering work of Britton Chance of the Johnson Research Foundation at the University of Pennsylvania in Philadelphia led to the establishment and development of the unique measurement technology and theoretical conceptualization of the mitochondrial function based on NADH redox state monitoring in vitro as well as in vivo.

The foundations for future NADH monitoring in vitro and in vivo were established mainly in the 1950s; thus this period will be discussed in this section.

Monitoring of NADH UV absorbance

In 1951, Theorell and Bonnichsen found a shift in the absorption spectrum of DPNH upon addition of alcohol dehydrogenase (238). In the same year, Theorell and Chance described a new spectrophotometric technique for measuring the formation and disappearance of the compound of alcohol dehydrogenase and NADH (239). In 1952, Chance showed the applicability of this new technique to the measurements of pyridine nucleotide enzymes of muscle homogenate or intact cells (25). In 1954, Chance and Williams briefly described new

sensitive differential spectrophotometric methods applied to the study of reduced NADH in isolated rat liver mitochondria and the same approach was used by Connelly and Chance (61) in monitoring NADH in stimulated frog nerve and muscle preparations. The oxidation of NADH in the muscle was similar to its oxidation in isolated mitochondria upon addition of ADP. In a comprehensive paper, "Enzyme mechanisms in living cells," Chance described in detail the measurements of the respiratory enzymes, including NADH (26).

A major milestone in NADH monitoring was the technique presented in 1954 by Chance (27) using a double beam spectrophotometer to determine the appropriate wavelengths in measurements of respiratory enzymes.

The detailed descriptions of the respiratory chain and oxidative phosphorylation in the mitochondria (published in 1955 by Chance and Williams) established our basic knowledge of the mitochondrial function (57). Chance and Williams defined, for the first time, the metabolic states of isolated mitochondria in vitro, depending on the substrate, oxygen, and ADP levels. In addition, they correlated those metabolic states to the oxidation-reduction levels of the respiratory enzymes. The physiological significance of those metabolic states was discussed in 1956 by Chance and Williams (58).

Monitoring NADH fluorescence

The fact that NADH was monitored by the difference in the absorption spectrum of its reduced form, limited the use of that technique to the study of mitochondria in vitro, and in very thin tissue samples (e.g., muscle) or in cell suspension. To provide a method more specific than absorption spectroscopy, fluorescence spectrophotometry in the near-ultraviolet range was applied for NADH measurement. The initial model of fluorescence recorder was described by Theorell and Nygaard in 1954 (240). The first detailed study using fluorescence spectrophotometry of NADH in intact Baker's yeast cells and algae cells was published in 1957 by Duysens and Amesz (75).

In the next 5 years (1958–1962), the monitoring of NADH fluorescence was significantly expanded, led by Chance and collaborators. In a first preliminary study, Chance et al. (37) performed simultaneous fluorometric and spectrophotometric measurements of the reaction kinetics of bound pyridine nucleotides (PN) in the mitochondria. In the same year (1958), Chance and Baltscheffsky presented preliminary results of measuring the fluorescence of intramitochondrial PN (34). In this study, they proved the connection between the mitochondrial metabolic state and the redox state of NADH as measured by spectral fluorometry in mitochondria isolated from rat liver (57). The correlation between the enzymatic assay of PN and sensitive spectrophotometry was investigated by Klingeberger et al. (120) by using the rat liver, heart, kidney, and brain.

In 1959, Chance and collaborators were able to expand the use of NADH fluorometry to various experimental models, from isolated mitochondria to intact tissue. To monitor NADH localization in intact cells, Chance and Legallais (42) developed a unique differential microfluorimeter with a very high spatial resolution. This approach was used in various cells to identify the intracellular localization of NADH fluorescence signals (54, 201). The next step was to apply the fluorometric technique to the higher organization level of animal tissues. Together with Jobsis, Chance measured in vitro changes in muscle NADH fluorescence following stimulation (41). In another paper published by Chance and Theorell (55) the authors came to the very significant conclusion that "The oxidation and reduction state of mitochondrial pyridine nucleotide without a measurable change of cytoplasmic fluorescence suggest that compartmentalization of mitochondrial and cytoplasmic pyridine nucleotide occurs in vivo, at least in the grasshopper spermatid."

An intensive use of the in vivo NADH monitoring approach started in 1962. The "classic" paper on in vivo monitoring of NADH was published in 1962 by Chance et al. (36). They were able to simultaneously monitor the brain and kidney of anesthetized rats using two microfluorometers. In 1962, Chance and collaborators elaborated on this kind of in vivo monitoring and used it in other rat organs (43, 50).

SCIENTIFIC BACKGROUND AND TECHNOLOGICAL ASPECTS

The absorption and fluorescence spectra of NADH (the reduced form) have been well characterized at different levels of organization, i.e., in solution, mitochondria and cell suspensions, tissue slices, and organs in vitro and in vivo. NADH has an optical absorption band at about 300 to 380 nm and a fluorescence emission band at 420 to 480 nm (Fig. 1, *B* and *C*). The spectra are considered the same, although there are small differences in the shape and maxima of the spectra for different environments and measurement conditions. However, there is a universal agreement that the intensity of the fluorescence band, independent of the organization level of the environment, is proportional to the concentration of mitochondrial NADH (the reduced form), particularly when measured in vivo from a tissue.

The biochemical and physiological significance of these spectral qualities is also universally accepted, that is, an increase in the fluorescence intensity indicates a more reduced state of NADH and of the rest of the mitochondrial electron transfer chain. Under various circumstances, changes in the redox state of the electron transport chain can be associated with various conditions.

To monitor NADH fluorescence, it is possible to use one of the two principles available. At the early stage, it was necessary to measure and identify the fluorescence spectrum of NADH. Fluorescence spectra were compared in different in vitro and in vivo preparations. In parallel, the second approach was adopted, namely, measuring the total fluorescence signal accumulated and integrated into a single intensity using appropriate filters. This approach was necessary to measure NADH fluorescence continuously. The following parts of this section describe the fluorescence spectra of NADH measured in various in vitro and in vivo models by different investigators. We present this review of the reported spectra to describe the foundations for the second monitoring approach, namely, the continuous monitoring of integrated spectra.

Fluorescence Emission Spectra of NADH

NADH in solution. Several investigators have measured NADH fluorescence in solution. Very recently, Alfano's group (62) performed a calibration test of pure β-NADH in solution, compared it to porcine myocutaneous flap, and found a very significant correlation. The NADH solution spectrum and mi-

tochondrial spectrum were also compared by Chance and Baltscheffsky (34).

Similar spectra of NADH in solution were recorded by Schomacker et al. (219) using 337-nm excitation light for colonic tissue diagnosis.

NADH spectra in isolated mitochondria. The excitation and emission spectra of NADH (PN) and flavoprotein were measured in frozen samples of pigeon heart mitochondria (52). Using rat liver mitochondria, Chance and Baltscheffsky (34) measured the fluorescence spectra in the three metabolic states defined by Chance and Williams (58). The 330-nm light excitation resulted in a fluorescence peak at 440–450 nm. The same kind of spectra was obtained by other investigators using different fluorometers or mitochondria isolated from various organs. Galeotti et al. (87) measured similar spectra from rat liver mitochondria. Using Rhodamine B as an internal standard for system calibration, Koretsky and Balaban (125) found the same spectra emitted from isolated rat liver mitochondria. Koretsky et al. (126) compared the emitted spectrum from heart homogenates (similar to isolated mitochondria) with that of dissolved heart homogenates (126).

Intact cells. The use of microfluorimetry to study intact cell metabolism was described in several publications by Kohen and collaborators (see, for example, Ref. 123).

The typical NADH fluorescence spectrum was measured in suspension of ascite tumor cells (87). This study demonstrated that the spectrum of intact cells was similar to that of NADH solution.

Using isolated myocytes, Eng et al. (78) compared the spectra measured under various conditions of the mitochondria. They found that cyanide induced an increase in the spectrum difference, whereas FCCP, used as a typical uncoupler of oxidative phosphorylation, produced a marked decrease in the spectrum.

Tissue slices and blood-free perfused organs. The next step in the development of NADH fluorometry, after its use in isolated mitochondria and single cells, was to apply it to tissue slices and isolated perfused organs in vitro.

The classic results of Chance et al. (36) were obtained from NADH in solution, in a suspension of mitochondria and in a perfused kidney slice. Only a very small spectral difference was found between the kidney slice, isolated kidney mitochondria, and the solution of NADH. The same type of comparison was performed by Aubert et al. (7) using a slice of the electric organ isolated from an electrophorus. The spectrum from the electric organ was very similar to pigeon heart mitochondria and NADH in solution. Chance (31) published more spectra originating from perfused rat heart exposed to various metabolic perturbations. A large, significant increase in the emission spectrum was recorded between normoxic and anoxic conditions, and between normoxic and amobarbital (Amytal)-treated hearts. These results suggested that when O_2 supply is eliminated (state 5) or when site I in the mitochondria is blocked by Amytal, a large change in NADH levels is recorded.

The same kind of normoxic-anoxic transition was found by Jamieson and Van den Brenk (103) using isolated gastrointestinal mucosa. The studies of Chance and collaborators were further expanded to isolated rat skin. The spectrum of the skin slice was very similar to that of the liver slice and NADH solutions. To test the responsiveness of the skin to metabolic manipulations, they compared spectra under normoxic and anoxic conditions. They also found a clear, significant increase in the skin spectrum under Amytal treatment (response not shown). Another organ of interest tested by Chance and Lieberman (46) was rabbit cornea (frozen) compared with rat liver mitochondria (states 2 and 4).

Other research groups adopted NADH fluorometry and tested the validity of its principles. For example, Koretsky et al. (126) employed rapid-scan video fluorometry, and found the same NADH spectrum when using excitation light from a N_2 laser (337 nm). Very recently, the spectrum of the hippocampal slice in vitro was measured by Perez-Pinzon et al. (200) and a marked increase in NADH spectrum was recorded under anoxia.

Organs in vivo. The use of NADH fluorometry for in vivo studies started at the end of the 1950s and has been presented in various publications. In a summative study, Chance compared spectra of NADH measured from rat kidney cortex to those of rat brain cortex and found that the main effect of anoxic transition, both in the kidney and the brain, was a large increase in the fluorescence intensity with no detectable shift in the spectra (36). Similar results were obtained by Chance (31) when intact sartorius toad muscle was stimulated. Stimulation of the muscle (state 4 to state 3 transition) led only to a decrease in the intensity of the fluorescence emission spectrum.

In 1975, Sundt and Anderson (232) applied in vivo fluorometry to study the brain of the squirrel monkey and recorded a greatly increased intensity in the dead brain as opposed to normal brain, with intermediate values in the ischemic brain. At the same time, Harbig et al. showed a clear increase in the NADH spectrum between normoxic and anoxic conditions in cat brain (93).

Corderio et al. (62) compared the excitation spectra in porcine myocutaneous flap with those of NADH in solution. Exposing the flap to 6 h of ischemia dramatically increased the intensity of 450 nm light. Furthermore, we compared two sources of excitation light: the usual mercury arc and laser excitation at 324 nm (152). The main problem in applying such spectra, under in vivo conditions, is the effects of hemodynamic changes under anoxia. To overcome this problem, we induced repetitive cycles of anoxia that suppress the autoregulatory compensation mechanisms (152).

Figure 1*C* shows six scans obtained from the normoxic (A1, A2) and the anoxic brain (B1, B2) using a Hg arc, and comparative scans using Hg (C1) and the laser source (C2) in the dead brain. The results indicate that the location of the emission spectrum peak is identical in normoxia and anoxia, and is close when the laser is used. We also used the laser source in several in vivo studies and found that the light intensity did not harm the brain during several hours of measurement. Under anoxia, a clear increase in NADH fluorescence spectra was recorded.

Comparison between NADH fluorescence intensity and biochemical analysis of pyridine nucleotides

To verify the source of NADH fluorescence signals monitored in vivo, it was necessary to freeze the monitored tissue and to biochemically measure its pyridine nucleotide content. Chance et al. (51) compared the fluorescent and analytical measurements of NADH and NADPH using in vivo liver. It

became clear that ischemia, limiting the availability of oxygen, led to a large increase in the fluorescent signal. At the same time, NADH showed a marked increase while NADPH remained unchanged. These results suggested that the source of the in vivo fluorescent signal is mainly from NADH. In 1966, Chance (31) summarized the studies comparing the fluorescence signals with the biochemical analysis of pyridine nucleotides. NADH was found to be the main source of fluorescence change in the in vitro beating heart. This held true under anoxia and under treatment with Amytal. Chance et al. showed a clear correlation between the fluorescence signal measured in the heart and the biochemical analysis of NADH in the tissue.

To test conditions where NADH becomes oxidized, the hyperbaric oxygenation effect was tested in the rat liver in vivo (40). NADH was found to be the main source for the increase of in *vivo* signal under Amytal treatment. Under hyperbaric hyperoxic conditions, the contribution of NADPH was larger. In the same study, Chance et al. (40) showed that in the brain cortex under anoxic or hyperbaric conditions, NADH was the main source of the fluorescence signal. In 1971, Jobsis et al. (110) compared the corrected NADH fluorescence signal (after subtracting the reflectance signal) to its concentration measured in a brain tissue sample after induction of convulsions or anoxia. A very clear correlation was discovered, but Jobsis et al. concluded, "a quantitative interpretation of the changes of fluorescence in terms of nanomoles of NADH and NADPH is not truly warranted at this point." Other investigators performed similar comparisons between the fluorescence signals and the analytical measurements. Shimazaki et al. (222) showed a good correlation between the fluorescence of NADH and its concentration in control cornea as well as in cyanide treated cornea. NADH fluorescence and enzymatically determined NADH levels were similarly compared in the brain subjected to ischemia (256). Toth et al. (248) found a clear correlation between the two parameters under various metabolic perturbations of the spinotrapezius muscle. In the in vivo muscle, cyanide treatment and ischemia caused an increase in both parameters while the glycolysis inhibitor IAA induced a decrease in both. The same effects have been found recently by Toth et al. (247) in tests of cat sartorius muscle in vivo. A significant correlation was found between the fluorescence signal change in ischemia and the amount of NADH determined enzymatically.

Intracellular origin of the NADH fluorescence signal

The intracellular localization of the signals measured from NADH had been discussed even before NADH fluorescence was measured. It is important to understand that the excitation and emission wavelengths of NADH (350 and 460 nm) are well separated from other endogenous chromophores, as described by Anderson-Engels and Wilson (4) and the 460-nm fluorescent emission originates primarily from NADH bound to mitochondria.

Klingenberg et al. (120), who used mitochondria from various organs, found that the sum of NAD and NADH was of the same order of magnitude in the liver, heart, kidney, and brain. Using mitochondria of rat liver and kidney, Avi-Dor et al. (10) came to the following conclusions: "The average fluorescence yield of reduced pyridine nucleotide in mitochondria is 6 to 8 times the yield of NADH and NADPH in aqueous solution." "The yield of mitochondrial NADH is substantially higher than the yield of mitochondrial NADPH."

The significance of these conclusions is that the in vivo fluorometric technique provides information about the redox state of NADH in the mitochondria with a negligible contribution of the cytoplasm. Estabrook arrived at the same conclusion using rat liver mitochondria, by comparing the fluorometric technique with the spectrophotometric approach (80). The same conclusion was drawn by Chance et al. (36) for rat brain and kidney in vivo, and by Jöbsis et al. (110) for cat brain induced to epileptic activity. Jöbsis and Duffield (108), using the fluorometric technique in intact toad sartorius muscle, concluded "that cytoplasmic NADH does not interfere materially with these measurements." A similar conclusion was reached by Chapman (60), positing that "mitochondrial NADH is the sole significant origin of labile fluorescence under the condition used." The same conclusion was reported later by Jobsis and Stainsby (112) for the mammalian skeletal muscle. O'Connor (193), who used in vivo monitoring of cat brain in combination with biochemical assays, stated the following: "The cortical fluorescence recorded with in vivo fluorometric techniques originated from mitochondrial NADH." The same results and conclusions were obtained by Nuutinen (190) using isolated perfused rat heart. Accordingly, "The NADH+NADPH fluorescence of the intact tissue originates largely from the mitochondria." In our own studies summarized in a review paper (152), we also confirmed the notion that most of the labile NADH signal in the brain originated from the mitochondria. Additional indirect evidence comes from other decapitation model studies performed by us (160, 259). We found that in the awake rat, the NADH fluorescence increase starts within 1 s and reaches its maximal level within $<$1 min. The same timing pattern has been described previously (53) when effects of decapitation were studied in anesthetized mouse brain. It has been reported (144) that after decapitation, a large enhancement of glycolysis occurs, but this may have started only several minutes after the decapitation. Lowry's findings also suggest that if NADH increases dramatically several minutes after the decapitation, it may derive from the cytosolic source. In no decapitated animal ($>$200 animals) did we ever find such a secondary increase in NADH fluorescence after the initial maximal increase. Eng et al. (78), studying single rat cardiac myocytes, asserted that "These data are consistent with the notion that the blue autofluorescence of rat cardiac myocytes originated from mitochondrial NADH." Very recently, Coremans et al. (63) confirmed that "The results show that the NADH fluorescence/UV reflectance ratio can be used to monitor the mitochondrial redox state of the surface of intact blood perfused myocardium."

Monitoring devices and technological aspects

Principles of NADH monitoring. As described in the introductory section, NADH can be measured by utilizing its absorption spectrum in the UV range, as well as by the blue fluorescence spectrum under UV illumination. In the early stages, NADH monitoring was based on the difference in the absorption of NADH and NAD^+. At the range of 320 to 380 nm, only the reduced form; NADH absorbs light, while NAD^+ does not (Fig. 1*B*). Therefore, when a mixture of NADH and NAD^+ is illuminated in a cuvette by 320–380 nm, only NADH

will affect the absorption spectrum peak at 340 nm. This property of NADH was used in the early 1950s by several investigators, as reviewed in *Spectroscopic Monitoring of NADH–Historical Overview*. Chance and collaborators utilized this technique to measure NADH in muscle homogenates or intact cells (25) and published many papers concerning the unique absorption spectrum of NADH.

The absorption approach is not practical for measuring NADH in a thick tissue; hence, another property of NADH was used. Since the early 1950s, fluorescence spectrophotometry of NADH has been employed in various in vitro and in vivo models. The emission of NADH fluorescence, under illumination at 320–380 nm, has a very wide spectrum (420–480) with a peak at 450–460 nm (Fig. 1*C*). NADH fluorescence has been identified by Chance and his collaborators as a good indicator of the intramitochondrial oxidation-reduction state (48).

Types of NADH fluorometers. Since the early 1950s, different groups have developed a number of fluorometers adapted to their specific experimental protocols. As of today, most of the groups using NADH fluorometers construct the devices in house, since no suitable commercial products are, in fact, available. During the past four decades, the workshop of the Johnson Research Foundation at the University of Pennsylvania Medical School (Philadelphia, PA), headed by Prof. Britton Chance, has manufactured a few types of laboratory instruments purchased and used by investigators (45).

The basic features of NADH fluorometers consist of the following: *1*) a light source (including appropriate filters); *2*) an optical path to the preparation and back to the detection unit; *3*) detection and signal processing units; and *4*) signal recording and storage units.

In our earlier review published in 1984, we extensively specified the light-guide-based fluorometry used in our studies (152).

The review article on in vivo NADH fluorescence monitoring, published in 1992 by Ince et al. (102) included many other technical aspects of the methodology. Nevertheless, here we will elaborate on the historical development of the various models of NADH fluorometers. We recently (155) reported on a new type of NADH fluorometer based on a very small and stable UV light source: a 375-nm light-emitting diode.

In the present review, we will not recommend the use of any type of fluorometer-reflectometer, but will rather provide the reader with extensive reference information, gathered during the years, on the construction of fluorometers. Priority will be given to articles mainly dealing with NADH monitoring in vivo, though in vitro fluorometer types will be also considered. Duysens and Amez (75) schematized the first fluorescence spectrophotometer used for intact cells. They utilized the classic light source (the mercury arc) providing a very strong band at 366 nm, even though not at the maximal NADH absorption peak (340 nm). Using a monochromator, they were able to obtain the NADH fluorescence spectrum in baker's yeast cells and photosynthesing cells. Duysens and Amaz concluded that "the fluorescence excited by 366 nm can be used for measuring reduced pyridine nucleotide in vivo".

In 1959, Chance and Legallais (42) described a differential fluorometer that heralded a new era in monitoring NADH fluorescence in vivo as an indicator of mitochondrial function. They used a microscope, serving as the fluorometer basis, with two light sources: tungsten and mercury lamps with appropriate filters. In 1959, Chance and Jobsis (41) proved that mechanical muscle activity is associated with NADH oxidation measured in excised muscle. This study was the bridge from the subcellular (mitochondria) and cellular (intact cell) monitoring approaches toward actual in vivo applications.

The first in vivo NADH monitoring device was presented in the early 1960s. At that stage, the effects of scattered light and tissue absorption due to blood were not taken into consideration when monitoring NADH fluorescence. The first detailed results of in vivo NADH fluorescence measurements were published in 1962 (36).

These classic papers described two microfluorometers that were modifications of previous designs (42, 54). This microfluorimeter type employed Leitz "Ultrapack" illumination, which had been used for many years by various groups until the appearance of UV transmitting optical fibers. To avoid movement artifacts, rats were anesthetized deeply and their heads were fixated in a special holder attached to the operation table. Numerous studies utilized the principles of the "Ultrapack" illumination system. The same instrumentation was used in other in vivo studies, including those of Chance's group (38, 43, 44, 59), Dora and Kovach's group (71, 92), Rievich's group (93), Jobsis and collaborators (108, 110, 111, 213), Gosalvez et al. (89), and Anderson and Sundt (5, 232). This is only a partial list.

Monitoring NADH fluorescence and reflectance. The effect of blood on NADH fluorescence was discussed early by Chance et al. (36). To monitor NADH in vivo, Chance's group had to avoid areas containing large blood vessels, which interfere with the emission and excitation light. The monitoring of a second channel in tissue fluorometry in vivo was reported by Chance and Legallais in 1963 (44). They showed that "changes due to the deoxygenation of oxyhemaglobin do not interfere with measurement of the time course of fluorescence changes in the tissue studies."

The addition of a second monitoring signal, namely, tissue reflectance at the excitation wavelength was reported in 1968 by Jobsis and Stansby (112). It was based on a previous model described by Jobsis et al. in 1966 (107). In two more papers by Jobsis and collaborators (110, 111), the measurement of 366-nm reflectance was used for the correction of the NADH fluorescence signal from the brain. The reflectance signal was subtracted from the fluorescence signal. The same type of instrumentation was used by various groups for the measurement of NADH in single cells (124) or in vitro preparations (13, 19).

Fiber optic fluorometer/reflectometer. To enable the monitoring of NADH fluorescence in unanesthetized animals or other in vivo preparations, a flexible means was needed to connect the fluorometer with the tested organ, for example the brain. This was achieved in 1972, when UV transmitting quartz fibers became available (Schott Jena Glass). We have used the light guide-based fluorometer for in vivo monitoring of the brain (48, 157) subjected to anoxia or cortical spreading depression. The historical development of light guide-based fluorometery-reflectometry is shown in Fig. 2. The original device functioned on the time-sharing principle (Fig. 2*A*), where four filters were placed in front of a two-arms light guide. Filters 1 and 3 enabled the measurement of NADH fluorescence, while filters 2 and 4 were used to measure tissue reflectance at the excitation wavelength. The reflectance trace

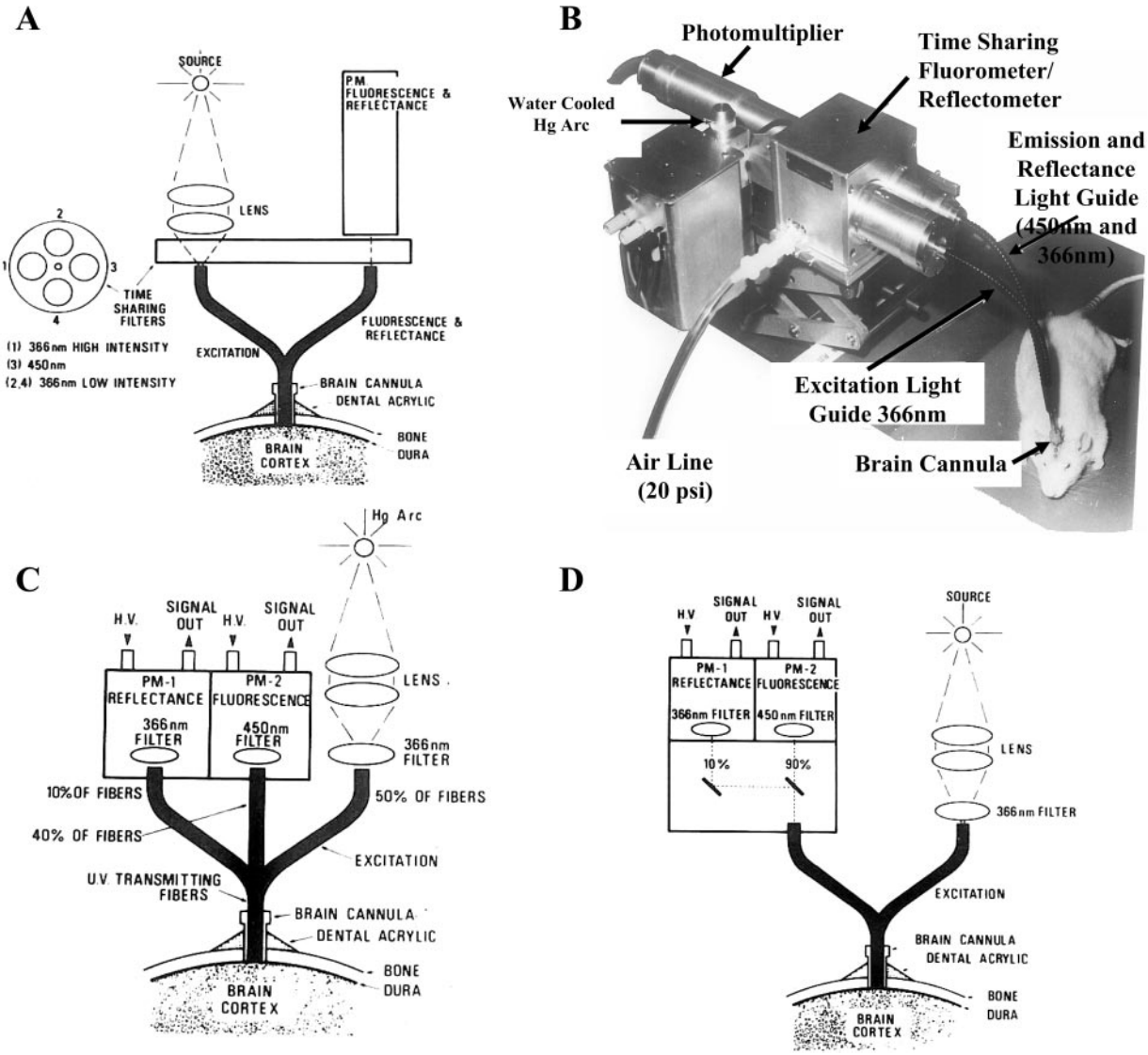

Fig. 2. The three stages in the development of the fiber optic fluorometer/reflectometer (started in the early 1970s).

was used to correct the NADH signal for hemodynamic artifacts, and to indicate changes in the blood volume of the sampled tissue.

In this original system, only one photomultiplier tube was used for the detection of the two signals. Figure 2*B* presents one of the first in vivo brain monitoring time-sharing setups, connected to the brain of an anesthetized rat (157). To simplify the monitoring system, the time-sharing approach was replaced by splitting the light emitted from the tissue into two unequal fractions for the measurement of fluorescence and reflectance signals. This model, named the DC type fluorometer, had a three-way light guide (Fig. 2*C*), which was later replaced by a two arms light guide probe (Fig. 2*D*). In all the three configurations, the reflectance signal was used for the correction of the fluorescence signal (see details in *Principles of NADH artifact correction*). The model shown in Fig. 2*A*, was used to study the brain (32, 157–159, 184) and kidney (84). The model shown in Fig. 2*C* was used to monitor the heart (47), brain (18), and kidney (84).

Our group developed and used the model shown in Fig. 2*D* in the late 1970s. This model is still being used in our laboratory to monitor the brain (148), heart (2, 114), liver (15), and kidney (178, 260), and in multisite or multiorgan monitoring (133, 156, 161).

Other groups used optical fibers to connect the monitored tissue to the fluorometer, differently than the three models shown in Fig. 2. Renault and collaborators used a light guide fluorometer for monitoring heart in vivo (206, 207). Rex and collaborators used another type of light guide fluorometer for the brain and other systems (202, 208). Microlight guides were used for in vitro and in vivo studies (104, 105, 244).

Principles of NADH artifact correction. In *Factors affecting NADH fluorescence and reflectance signals*, we will discuss the effects of various factors on the measurement of NADH fluorescence and tissue reflectance. To compensate for NADH unrelated factors, various approaches have been developed. In the paper published by Ince et al. (102), the various correction techniques are listed and discussed in detail. It appears that the

correction technique is also dependent on the instrument configuration (13, 93). Most of the published materials are based on the 1:1 ratio, when subtracting the 366-nm reflectance from the fluorescence signal. As of today, a new approach is still lacking to compensate for non-NADH factors affecting the NADH fluorescence signal. We have found that subtracting the reflectance from the fluorescence or dividing the two parameters provides similar net NADH changes. Very recently, Bradley and Thorniley (20) published a review article dealing with the various correction techniques for tissue fluorescence. They summarized their review by the following conclusion: "even though research has been conducted into correction techniques for over thirty years, the development of a successful and practical correction technique remains a considerable challenge."

Calibration of the monitored signals. To reduce the variation between different animals in a specific protocol, a standard procedure for signal calibration was used by various investigators. Since NADH could not be calibrated in absolute NADH concentrations, it was necessary to use a calibration procedure before each experiment. Different groups had developed standard procedures for calibration.

Because the technology is rapidly changing, it is unnecessary to use the old approaches for signal calibration. Ince et al. (102) listed the various calibration procedures. As an example, we will present the calibration procedure used in our laboratory before a new computerized system was integrated in our fluorometer. The reflectance and fluorescence signals obtained from the photomultipliers (RCA 931B) were calibrated to a standard signal (0.5 V), as recently described in detail (161) by variation of photomultiplier dynode voltage obtained from a high-voltage power supply. The standard signal (0.5 V) used to calibrate the recorder was set to give a half-scale deflection on the recorder (2.5 cm) with the pen resting at midscale. The gain was increased, as required, by a factor of 2 or 4 to give 50% or 25% of the full scale correspondingly. The changes in the fluorescence and reflectance signals were calculated relatively to the calibrated signals under normoxic conditions. This type of calibration is not absolute but provides reliable and reproducible results from various animals and also among various laboratories using this approach.

FACTORS AFFECTING NADH FLUORESCENCE AND REFLECTANCE SIGNALS

The excitation and emission spectra of NADH are affected by the redox state of this fluorochrome and by other factors, leading to artifacts in the fluorescence measurements. This section will discuss various NADH-unrelated factors, affecting the measured signal. Since most fluorometers involve the measurement of the total backscattered light at the excitation wavelength (i.e., 366 nm), the discussion will concern changes in NADH fluorescence as well as in tissue reflectance.

The following factors may affect the two measured signals, 366-nm reflectance and 450-nm fluorescence: *1*) tissue movement due to mechanical or intracranial pressure changes; *2*) extracellular space events, such as volume changes or ion shifts between intra- and extracellular space; *3*) vascular and intravascular events, for example, oxy-deoxy Hb changes, and blood volume changes due to autoregulatory vasoconstriction under pathological conditions; and *4*) intracellular space factors, such as O_2 level, ATP turnover rate, substrate availability, and mitochondrial redox state. This subject will be discussed later on.

The effects of factors 1–3 will be discussed below and factor 4 in *Changes in mitochondrial NADH and metabolic state*.

NADH UNRELATED FACTORS

Movement artifacts. Using the fiber optic technique, we found that when there is a good contact between the bundle of fibers and the monitored tissues, such as the brain, all movement artifacts are eliminated. We also found that to obtain a good signal-to-noise ratio, as well as a reliable and repeatable measurement, good contact between the fibers and the tissue is required during the entire monitoring period. If a small space is left between the fibers and the tissue, the signal will not be greatly affected but responses will not be observed. Pressure on the brain must be avoided, and we solved this problem by using a special light guide holder cemented to the skull (157, 159). In monitoring other organs, a micromanipulator can be used to hold the light guide above the organ (133, 161). In the heart, this problem has been solved by using a light guide-holding cannula connected to the heart muscle by three sutures (114, 115, 195). In brain preparations, even while the animal was undergoing hyperbaric convulsions or decapitation, only very small artifact changes in the traces were measured from the brain, indicating that the movement has only a negligible effect on NADH measurements. The same approach was applied previously (68, 70–72), in anesthetized and/or artificially ventilated rats or cats, using the "Ultrapac" optics for brain monitoring. Another option is to glue a light guide holder by cyanoacrylate glue, when monitoring exposed organ surfaces (15, 178).

To avoid movement artifacts in monitoring patients, we used diverse approaches. In the neurosurgical intensive care unit, we used a metal holder screwed to the skull of comatose patients (162). In the operating room, we used a floating light guide probe fixed to the head holder in neurosurgical procedures (164) or a ring used to hold retractors during abdominal operations or kidney transplantations (178).

Intra- and extracellular space events. The second factor, which can be a potential source of error in NADH fluorescence measurement, is a change in the absorption properties of the tissue, during various perturbations, at the observed site. This artifact has been recognized mainly in brain studies. Very little is known and published about this factor, due to the inability to separate it from other factors affecting the NADH fluorescence readings. It seems to us that under physiological or pathological conditions involving ions and water movement between the intracellular and the extracellular space, this factor may have a greater effect on NADH fluorescence measurements. We have earlier published indirect evidence for the involvement of this factor in our measurements and a possible correction method.

First, when the blood was eliminated from the brain, using a fluorochemically perfused brain preparation (174), only very small, if any, changes in reflectance were measured during the anoxic cycle. As shown in Fig. 4*B*, the uncorrected NADH fluorescence and the corrected fluorescence (CF) had similar kinetics. Furthermore, the CF response of the perfused brain to anoxia was similar to that of the blood-perfused brain in the

same animal before the initiation of perfusion shown in Fig. 4*A*. However, when a spontaneous spreading depression (SD)-like response was recorded in several perfused brains, the reflectance tracing showed a change typical of the initial increase phase of the regular response to SD found in a normoxic blood-perfused brain (for details, see Ref. 174). The second phase of the decrease in reflectance during SD did not occur in the perfused brain due to the lack of blood in the system. We believe that this initial increase in reflectance was due to water and ion movement during the SD event in the perfused brain. The same type of reflectance response (an increase) was obtained when a brain slice in vitro was stimulated (142).

Second, an interesting correlation was found between the reflectance trace and P_{O_2} monitored from the gerbil brain subjected to spreading depression (169). In the awake state, the biphasic change in reflectance under SD was recorded as described here. However, under deep anesthesia, the two phases were separated, and the initial increase was not correlated to P_{O_2}. The second decrease in reflectance was directly correlated with the changes in P_{O_2} that resulted from blood volume alterations during SD. It seems that this initial increase phase of reflectance is also due to water and ion shifts during the initiation and propagation of the SD wave and is not correlated to the recovery phase.

Finally, in experiments where complete cerebral ischemia was induced by decapitation in rats and gerbils (259), bilateral carotid occlusion in gerbils (166), or 4-vessel occlusion in rats (163), a large reflectance increase was recorded after NADH reached its maximum level ($P_{O_2} = 0$). This increase was termed secondary reflectance increase (SRI). In recent experiments, we have monitored the DC potential as well as K^+ from the extracellular space, together with NADH fluorescence and 366-nm reflectance. In all cases, we found a very significant correlation between the complete depolarization occurring during complete ischemia (as identified by the DC and K^+ changes) and the SRI phenomenon. In few decapitated animals we found that during the appearance of the SRI, the corrected NADH signal decreased meaning that oxidation of NADH without the availability of oxygen. It seems that the SRI is partly due to the water and ion movements during the complete depolarization, and it may also be due to a decrease in tissue blood volume as a result of a spasm of blood vessels. In several cases, the SRI was very large (significantly) and the regular correction technique was insufficient. We have found that under partial ischemia in gerbils, with SRI occurring, a decrease in blood flow and P_{O_2} was recorded, indicating a possible massive vasoconstriction response that might be responsible for the SRI. One may argue that the continued fall in the NADH (oxidation) after the initial increase in NADH, due to the lack of O_2, is due to the loss of mitochondria via apoptotic cell death or other cell death mechanisms as suggested by Riess et al. (209) or Varadarajan et al. (252) in studying the preconditioning of the heart. We are sure that this is not the case in our system. We showed that even when complete ischemia was induced in gerbils for 30 min, the NADH signals were recovered to the baseline levels and the response of the recovered brain to cortical spreading depression was identical to that recorded before the ischemia (166). These results suggest that even during 30 min of ischemia, including the SRI, the integrity of the mitochondria was not damaged.

Vascular events. These events include changes in blood oxygenation, namely in the saturation level of HbO_2, as well as changes in the blood volume in the monitored microcirculation.

Blood oxygenation. Since hemoglobin (Hb) is a strong light absorber at various wavelengths, the measurements of NADH are affected by the amount of Hb in the monitored tissue. Kramer and Pearlstein (132) attempted to use the hemoglobin isosbestic point (448 nm) to correct the NADH measurement for changes in the [Hb]/[HbO] ratio. However, the attempt was unsuccessful and without any continuation, since their paper only presented preliminary results. To test the effect of Hb concentration in the tissue on NADH fluorescence spectrum, Rahmer and Kessler (204) used perfused rat liver and found that higher concentrations of Hb corresponded to a lower intensity of the fluorescence spectrum emitted from the liver.

Very recently, Coremans et al. (63), in their measurements of NADH fluorescence and light reflectance (365 nm), tested the effects of NADH and hemoglobin on the two signals in a tissue phantom model. They concluded that the ratio between the two signals (F/R) provides a good corrected signal.

In transition from oxygenated blood (HbO_2) to deoxygenated blood, the absorption spectrum is different and may affect the NADH signal. The oxy-deoxy Hb transition and its effect on the measured signals have been discussed previously (48), and this effect has been shown to be negligible. Indirect studies produced the following similar results. First, in decapitation, only a small change, if at all, was measured in the reflected light, although the hemoglobin present in the measured field was rapidly losing O_2. This indicates that the oxy-deoxy Hb transition has only little effect on NADH fluorescence and on the reflected light. Second, in comparing the normoxic-anoxic transition to the anoxic-normoxic one (induced by breathing N_2), the different kinetics in the reflectance traces suggest that blood oxygenation does not have a significant effect on the CF, when using 366-nm reflectance changes for correction. The decrease in reflectance after initiation of anoxia has very fast kinetics (it takes <1 min to reach the minimum reflectance level). However, during reoxygenation, the CF has very fast kinetics, and it takes 5 min or more for reflectance to reach the baseline. This indicates that the oxy-deoxy transition has only little effect on the two measured signals (reflectance, fluorescence).

Finally, in our previous publications (157, 159), we have shown that during anoxia in a normal rat, a two-step decrease in reflectance occurs. First, there is a small decrease in reflectance, which is followed by a very large decrease when NADH reaches its maximum level. This secondary decrease in reflectance during anoxia did not appear if the brain had been made partially ischemic by bilateral carotid artery occlusion for 24 h. The corrected fluorescence (CF) responses, however, were about the same. Furthermore, when N_2 cycles of 1 min were applied to the same rat every 10 min, we found that the reflectance responses decreased in time, while the corrected fluorescence showed the same response to anoxia (157). This occurred even though the oxy-deoxy hemoglobin change probably took place in all N_2 cycles.

Blood volume changes. Blood volume changes may occur as a response to various physiological and pathological condi-

tions. This is the main artifact in monitoring tissue NADH fluorescence, and it has been discussed by many investigators. During the past 30 years, we have used fiber optic surface fluorometry to monitor the brain exposed to various conditions, as well as other organs such as the heart (114, 189). Hence, evidence for the involvement of blood volume artifacts and their correction have been drawn from various published experiments.

First, the typical decrease in reflectance during brain anoxia can be corrected to a level of 90–100% depending on the microcirculatory pattern of the site under observation. When hemoglobin was eliminated from the brain (perfused with a fluorochemical), no blood volume changes could occur, and indeed no changes in reflectance were observed (174). In the heart, anoxia did not have a great effect on reflectance and the observed change was in the same direction as in the brain (114). In a partially ischemic brain (147) or when N_2 cycles were repeated many times (157), the typical decrease inreflectanceduring anoxia was also minimal, due to the low brain capacity to increase its blood volume to compensate for low P_{O_2}.

Second, in another set of experiments, we monitored NADH during hyperbaric oxygenation of the brain (167, 177). We found that when the animal was exposed to compressed 100% O_2, a large increase inreflectancewas recorded. This was explained by a decrease in blood volume in the brain due to the vasoconstrictive response of the blood vessels to high P_{O_2}. When the compression mixture contained 1.5% CO_2 at 5–6 ATA, the reflectance trace showed a sharp decrease due to the vasodilation response occurring under high P_{CO_2}. The CF showed the same level of oxidation. This shows that CF can be corrected for blood volume changes induced by high P_{O_2} or high P_{CO_2} in the brain, using the 1:1 subtraction technique.

Third, in studying the effects of unilateral or bilateral carotid artery occlusion in gerbils, the observed reflectance changes were in the same direction (169). Under unilateral ischemia induction, the reflectance trace showed a small decrease (or no change) due to the increase in blood volume through the open artery. However, when complete ischemia was induced (by additionally occluding the other artery), an increase in reflectance was recorded in the preparations. This indicates that a decrease in blood volume may lead to the expected increase in reflectance.

Finally, a decrease in blood volume was induced by saline injection into the ipsilateral common carotid artery or into the brachial artery (Gyulai and Mayevsky, unpublished results). The results showed that the increases in reflectance and fluorescence were similar and varied in the range of 10–20% between various rats or in the same animal.

Changes in mitochondrial NADH and tissue metabolic state

The pioneering work of Chance and Williams in the 1950s, led to the definition of the metabolic state of isolated mitochondria in vitro. The foundations for the use of NADH fluorescence as a marker of mitochondrial activity have been posited in detail by Chance and Williams (56, 57). The left portion of Fig. 6 is a modification of a published table, while the right hand segment demonstrates the responses of NADH fluorescence measured in the brain in vivo under various perturbations. The "resting state" of the mitochondria in vitro was defined as state 4, where NADH was 99% in the reduced form, and ADP was the rate limiting substance. If ADP is added to a suspension of mitochondria, ATP synthesis will be stimulated, O_2 consumption will increase, and the rate limit will be determined by the activity of the respiratory chain. During this state 3, or the "active state," the NADH redox state will decrease or become more oxidized (~50%). When the resting mitochondria are deprived of O_2, the activity of the mitochondria will stop and NADH will reach its maximum redox state (state 5).

A definitive description of the mitochondrial metabolic state has never been given for in vivo conditions. Therefore, we described the in vivo mitochondria conditions as recorded by NADH fluorescence in a representative tissue or organ; e.g., the brain. While the range between minimal NADH (~0) and its maximal level was determined in vitro, it is almost impossible to determine in the intact brain or other organs in vivo. For example, state 2, with a substrate free medium, could not be achieved in vivo since the tissue would die. On the other hand, the maximal level of NADH (state 5) could be monitored in vivo under complete deprivation of O_2 by anoxia or complete ischemia.

We used changes in NADH levels monitored in vivo to create a new scale ranging from a maximal definite point to the minimal level recorded in vivo. Details of this approach have been published (152). As shown in Fig. 3, the maximal NADH level is achieved under complete O_2 deprivation that can be induced both under in vitro and in vivo conditions. This signifies that this definitive point can be used to determine state 5 in vivo as well. The problem is to determine the metabolic state of a tissue in an in vivo situation. If we adopt the in vitro value of a resting state (state 4), this would signify that the increase in NADH during state 5, induced by anoxia (0% O_2), would be only 1%. According to all in vivo studies, this is not the case, and during anoxia the increase in NADH is lager than the decrease under state 4 to 3 transition. Figure 3, *right*, illustrates that the observed level of NADH increase is indeed larger than the decrease. Therefore, we concluded that, under

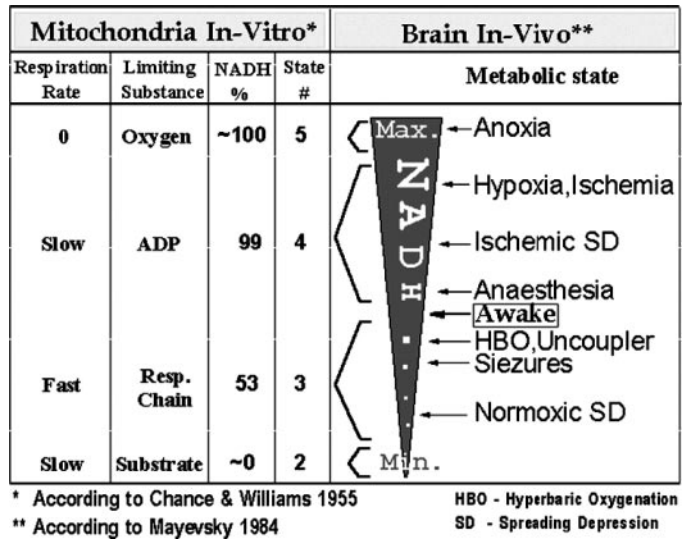

Fig. 3. Comparison between the mitochondrial metabolic state, defined by Chance and Williams (56, 57) and responses of the in vivo brain to changes in O_2 supply and brain activation.

in vivo conditions, the "resting" metabolic state of the brain is found between states 4 and 3 rather than in state 4 as defined in vitro (152). To determine the maximal and minimal levels of NADH in vivo it is almost impossible to use cyanide or uncoupler (FCCP). Nevertheless, we were able to determine the maximal level by anoxia and the "minimal" level by nonfluorescing uncoupler. We injected the uncoupler pentachlorophenol into the ventricles of the rat's brain while monitoring the NADH responses to anoxia and spreading depression (146). To perform a reliable study with cyanide, the animal would have to die and the results will not be helpful; therefore, we used the anoxia response to measure the maximal level of NADH. Using fiber optic fluorometry, we were able to monitor both anesthetized and awake rats. This figure will be discussed later on in this review. It is important to note that most of the published data on NADH monitoring, have been accumulated in brain studies. Therefore, we will present our data mainly relating to the brain, though results on other organs will be presented as well. Table 1 lists studies published by various investigators as well as our publications. The papers are classified according to the organ monitored and the type of perturbation used. This table does not include rarely studied types of organs or perturbations. Such studies are cited individually in the text.

Perturbation of O_2 supply in vivo. As described by Chance and Williams (57, 58), the complete depletion of O_2 from the mitochondria inhibits oxidative phosphorylation and terminates ATP production. This situation destroys the normal function of the tissue, and cell death can ensue. In this review, we define anoxia as a complete deprivation of O_2 caused by breathing 100% N_2. Hypoxia implies that the deprivation of O_2 from the breathing mixture is partial and ranges between 21% (normal air) and 0% (anoxia). Ischemia is defined as a decrease in O_2 supply due to a decrease in blood flow to the monitored organ. The degree of ischemia can vary from a full absence of flow (complete ischemia) to various levels of blood flow (partial ischemia). Although O_2 deficiency is the main event in each of the three experimental conditions (anoxia, hypoxia, and ischemia), other physiological factors may differ. For example, microcirculatory blood flow is decreased under ischemia, but increases under brain hypoxia. Thus, changes in the tissue due to other blood flow related factors are not identical.

ANOXIA AND HYPOXIA. The responses to hypoxia and anoxia are very similar; therefore, they will be discussed together. According to the definition of Chance and Williams (56, 57), a shift toward state 5 involves an increase in NADH proportional to a decrease in O_2 supply.

It is assumed that the response of NADH fluorescence to hypoxia or anoxia, induced in vivo, should be very similar to the response of isolated mitochondria. As shown in Fig. 4*B*, when the blood-free brain was exposed to N_2, the fluorescence showed a clear increase-decrease cycle depending on the availability of O_2. The reflectance trace was not affected at all. In autoregulated blood-perfused organs, it is expected that the lack of O_2 will trigger compensation mechanisms that may lead to an increase in the blood flow and volume, or a decrease in thereflectancesignal. We tested, in the same rats, the response to anoxia of the normoxic blood-perfused brain. The results are shown in Fig. 4*A*. Indeed, reflectance exhibited a large decrease due to the increase in blood volume (vasodilatation of brain vessels). Figure 4, *C* and *D*, presents the responses to anoxia measured via 2 mm and 1 mm light guides. A small variation can be seen in the reflectance response between the two light guides.

This mechanism is not active in all tissues and therefore different responses of the reflectance signal may be recorded in different tissues. Figure 5 shows the responses of a puppy dog brain to graded hypoxia (*A–C*) as well as to brain anoxia (*D*). As it is shown, the changes in the corrected fluorescence signals (CF), which represent the NADH redox state, were inversely correlated to the decrease in FiO_2 levels (from 6% to 0% O_2).

Figure 6 presents the responses of four rat body organs to graded hypoxia and anoxia. The four organs (the brain, liver, kidney, and testis) show very similar responses to the decrease in O_2 supply to the rat. Although the four organs were exposed to the same level of O_2 supply, the magnitudes of changes were not identical. Nevertheless, the NADH responses to hypoxia and anoxia clearly show that NADH fluorescence is a good indicator of O_2 supply to any of the four organs in the body. Table 1 lists the reports about the effects of anoxia or hypoxia on NADH in various organs. The brain studies were done in vivo, whereas the listed reports on other organs also include several in vitro studies. In our experiments, we have used a

Table 1. *Effect of O_2 delivery and consumption on NADH redox state measured in various intact organs by various investigators*

	Anoxia-Hypoxia	Ischemia
Brain	8, 18, 32, 36, 43, 44, 48, 53, 68, 73, 85, 93, 99, 106, 109, 130, 134, 135, 147, 148, 152, 156, 157, 159, 163, 169, 170, 179, 180, 183, 185, 205, 223	5, 16, 35, 53, 85, 95, 96, 113, 146–148, 150, 152, 154, 156, 160, 163, 165, 166, 169–171, 174, 176, 182, 183, 187, 221, 232, 246, 256, 258, 259
	SD-Cortical Spreading Depression	*Hyperoxia + HBO*
	85, 146, 147, 152, 157–159, 163, 164, 169, 170, 173, 174, 176, 181, 228, 229	148–153, 167, 177, 212
	Anoxia-Hypoxia	Ischemia
Heart	16, 17, 24, 30, 47, 59, 91, 114, 189, 194, 196, 207, 227	2, 16, 17, 21, 22, 35, 86, 101, 115, 116, 189, 196, 206, 207, 209, 210, 216, 230, 252
Liver	51, 53, 104, 105, 118, 122, 161, 218, 230, 245	15, 35, 51, 53, 119, 242, 243
Kidney	3, 12, 13, 32, 53, 84, 117, 121, 122, 161, 203, 260	3, 53, 64, 84, 117, 175, 178, 242
Skeletal muscle	28, 29, 109, 112, 257	109, 112, 198, 247, 250
Gastrointestinal tract	29, 103, 145	11, 211
Spinal cord and PNS	23, 65, 237	109, 224

Reference numbers related to cortical spreading depression (SD) on hyperoxia (HBO) are shown for the brain. PNS, peripheral nervous system.

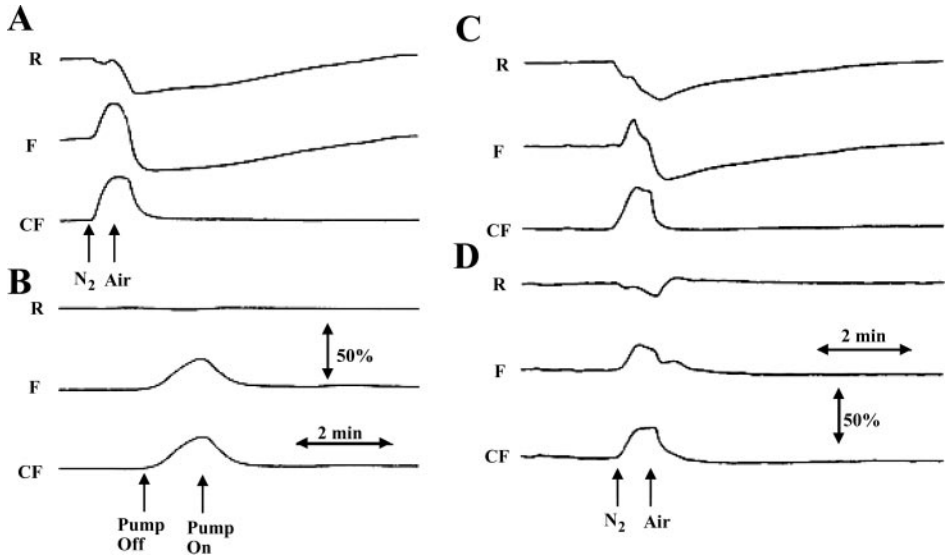

Fig. 4. Responses to O_2 deficiency measured in blood-perfused brain (*A*) and fluorochemical-perfused brain (*B*). The effect of the monitored tissue volume (the diameter of the fiber optic probe) is shown in *C* (2 mm diameter) and *D* (1 mm diameter).

short anoxic episode (20–30 s) to test the intactness of the tissue. If the NADH response to anoxia was too small, we stopped the experiment, because it indicated that the brain was damaged and NADH was already elevated. Accordingly, the number of responses to anoxic episodes is very large, and only representative references are cited.

ISCHEMIA, OR DECREASED BLOOD FLOW. Under partial or complete ischemia, blood flow to the monitored organ is decreased and, as a result, O_2 delivery is limited or even abolished. The use of ischemia in animal models provides information relevant to critical clinical situations such as brain stroke or heart attack. The primary factor starting the pathological state is the decrease in O_2 supply, making the tissue energy balance negative, and preventing the tissue from performing its function. Figure 7 illustrates the effects of ischemia and anoxia on the NADH level in the brain of an anesthetized gerbil. The measurements of NADH in the cerebral hemispheres were correlated to the brain electrical activity (ECoG; electrocorticogram). To test and compare the measurements done in the two hemispheres, we exposed the gerbil to short-term anoxia. As shown, the two responses are very similar and correlate to the depression of the ECoG signal measured in the two hemispheres.

The reflectance trace shows a typical decrease due to the increase in blood volume in the monitored site. The NADH (CF) showed a significant increase, which recovered to the baseline after resuming air breathing. Unilateral ischemia in this specific gerbil led to an increase in NADH in the ipsilateral hemisphere, while the contralateral hemisphere was not affected at all. ECoG also responded only in the occluded hemisphere. In part B, the left common carotid artery was occluded and in C, the right carotid artery was occluded. The effect of the blood volume changes, measured by the reflectance trace, was very small in the gerbil, and as a result, the

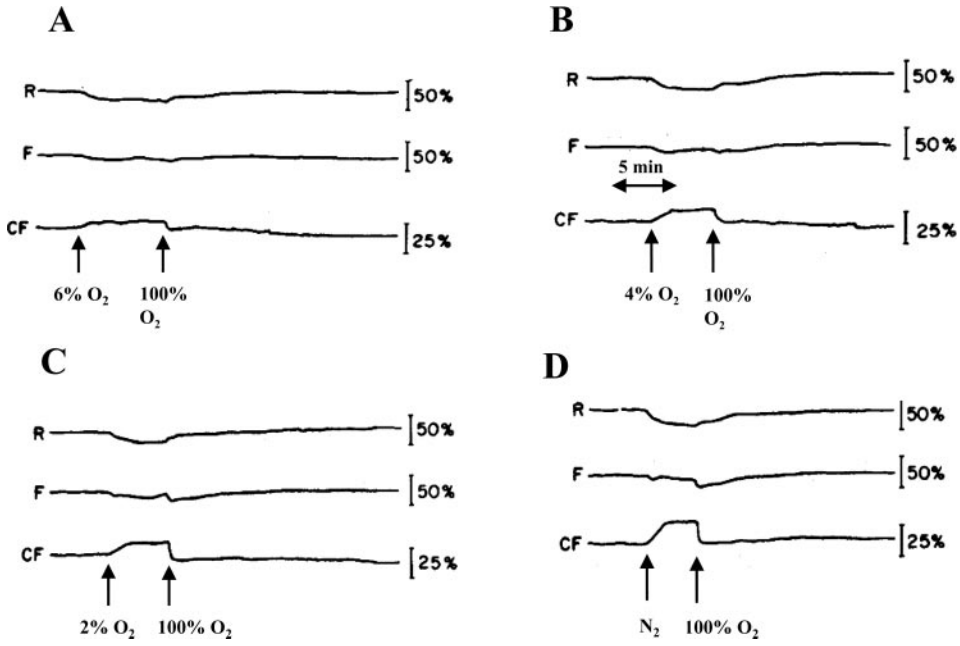

Fig. 5. NADH responses to graded hypoxia induced by exposing a dog puppy to 6% (*A*), 4% (*B*), 2% (*C*), and 0% (*D*) O_2.

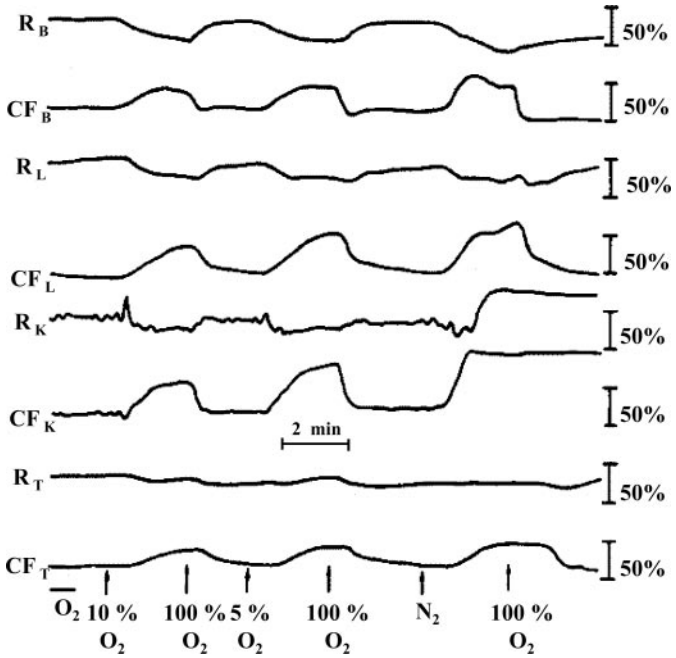

Fig. 6. Effects of hypoxia (10% O_2 and 5% O_2) and anoxia (100% N_2) on NADH fluorescence and tissue reflectance measured in four organs of an anesthetized rat. R_B, R_L, R_K, R_T: reflectance of the brain, liver, kidney and testis, respectively. CF_B, CF_L, CF_K, CF_T: corrected NADH fluorescence of the brain, liver, kidney, and testis, respectively.

fluorescence signal and the corrected fluorescence signal (CF) were very similar. In this specific gerbil, the connection between the two anterior cerebral arteries was minimal and, therefore, no blood compensation between the two hemispheres was noted (183).

Figure 8 presents the responses of a dog heart to lack of O_2, monitored in vivo by a fiber optic fluorometer-reflectometer. In parts A and B, the dog was exposed to a short (Fig. 8*A*) or a longer anoxic episode. In the two anoxic episodes, the NADH was elevated significantly. In the second anoxia, the heart went into fibrillation (Fig. 8*B*) and the dog died. In Fig. 8*C*, the coronary artery occlusion led to a very large increase in NADH while the change in the reflectance signal was very small. The changes in blood flow measured by a laser Doppler flowmeter were typical for an ischemic event, as expected. Publications on the effects of ischemia on NADH fluorescence in various organs are listed in Table 1. In all animals or organs used, the NADH was elevated in proportion to the level of ischemia.

HYPEROXIA, OR NORMOBARIC AND HYPERBARIC INCREASE IN P_{O_2}. To expose an organ in vivo to elevated oxygenation, it is possible to use one of the two options. First, normobaric hyperoxia is achieved by making the animal breathe elevated FiO_2, namely between 21% O_2 to 100% O_2 at atmospheric pressure. Second, hyperbaric hyperoxia is induced by using a hyperbaric chamber, in which O_2 pressure is elevated while the animal is located in the chamber.

It is well documented that providing animals or man with elevated oxygenation will terminate in the development of "oxygen toxicity." The time needed for the development of this toxic event is inversely proportional to the level of oxygenation, namely the higher the P_{O_2}, the shorter the time.

On the other hand, providing more O_2 may be beneficial in conditions such as carbon monoxide toxicity, body oxygenation pathology (heart or lung problems), and severe trauma. Therefore, it became necessary to understand the relationship between the level of oxygenation and the function of the mitochondria in vivo.

In the mid-1960s, Chance and collaborators (31, 39, 40) developed the experimental setup that enabled the exposure of various types of mitochondria as well as of the entire small animal in the hyperbaric chamber. They showed that the NADH of the brain, liver, and kidney became oxidized under hyperbaric oxygenation, and this effect was correlated to a decrease in pyridine nucleotides measured by biochemical analysis of fixed tissue.

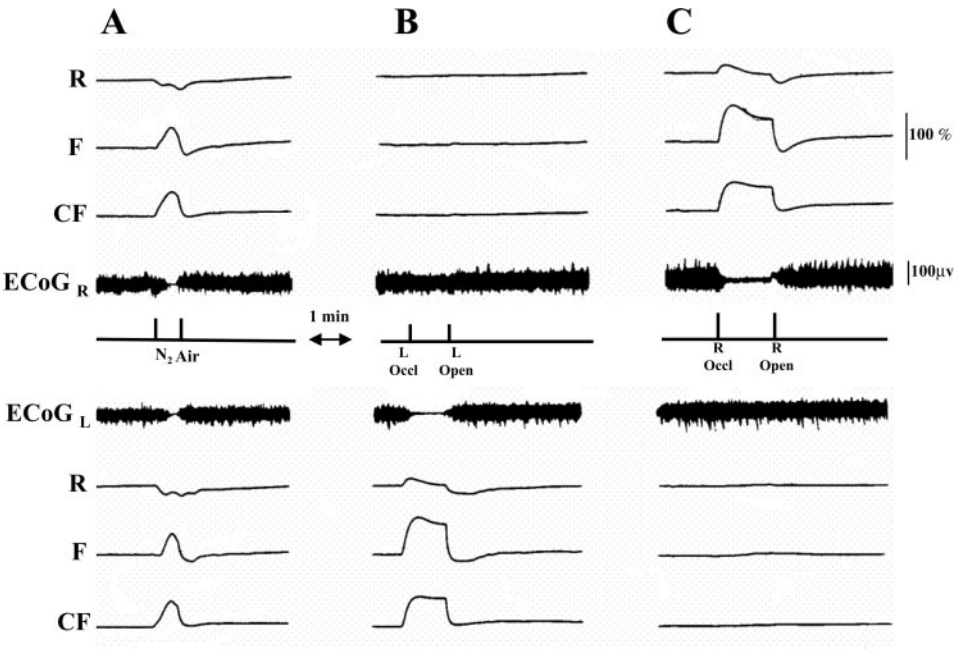

Fig. 7. Responses of the gerbil's brain to anoxia (*A*) and partial ischemia induced by occlusion of the left carotid artery (*B*) or right carotid artery (*C*).

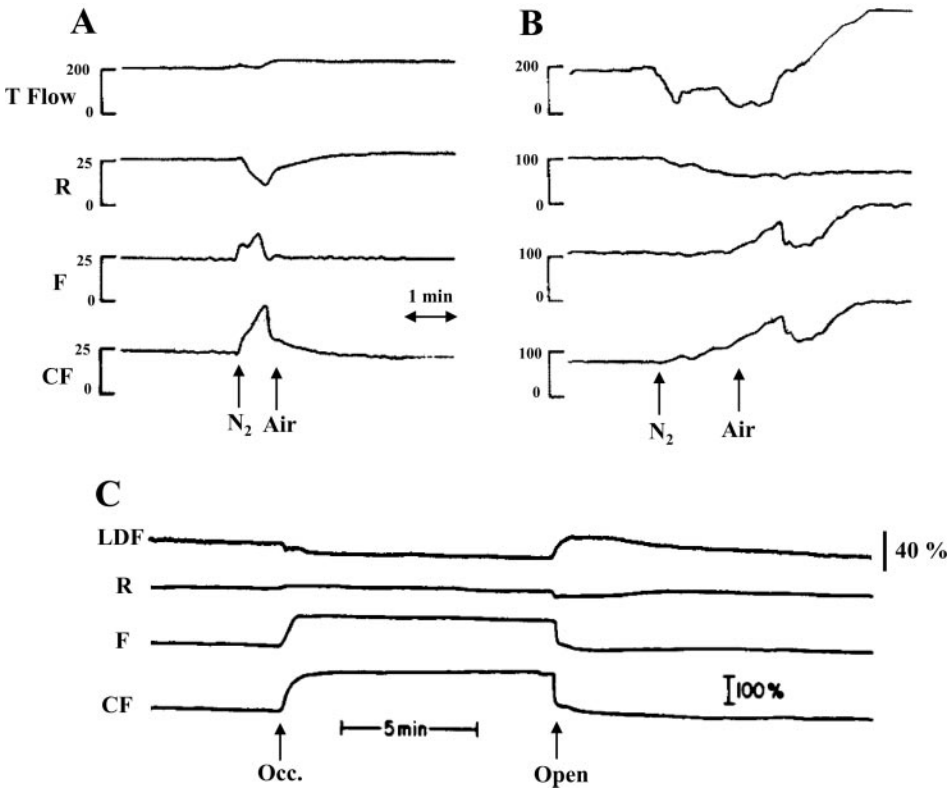

Fig. 8. Effects of anoxia (*A* and *B*) and ischemia (*C*) on the NADH redox state and tissue blood flow in the dog heart in an open chest preparation. T flow and laser Doppler flowmeter (LDF): monitoring of microcirculatory blood flow by heat clearance and laser Doppler flowmetry, respectively.

After the introduction of the light guide-based fluorometry, we were able to expose the awake brain to hyperbaric conditions. A clear decrease in NADH (oxidation) was recorded during the shift from 21% to 100% O_2, as well as during compression of up to 10 atmospheres 100% O_2 (150, 152, 153, 167, 177). A similar oxidation was found upon CO_2 addition to the gas mixture (94–99% O_2) (149). We also found a correlation between the elevated brain P_{O_2} and the oxidation of NADH in awake rats (151). The oxidation of NADH was also recorded under normobaric hyperoxia (113). Furthermore, we tested the effects of hyperbaric oxygenation on carbon monoxide intoxication (212) or cyanide exposure (235).

CHANGES IN INSPIRED CO_2 AND CO. The involvement of CO_2 in tissue energy metabolism has been studied by several investigators, using higher (hypercapnia) or lower (hypocapnia) CO_2 levels in the gas mixture. In 1968, Granholm et al. (90) showed that hyperventilation of a rat led to an increase in NADH probably due to a decrease in cerebral blood flow. Using the monkey brain, Sundt and Anderson (231) and Sundt et al. (233) tested the effects of hyper- and hypocapnia on NADH responses in normoxic and ischemic tissue. No change in NADH was found in the normoxic brain, whereas in the ischemic brain, the change in P_{CO_2} did not affect the elevated NADH. They found a decrease in NADH during seizures, however, nonconcomitant with CO_2 changes (236). Under hypocapnia, there was an increase in brain NADH due to a decrease in cerebral blood flow (18, 205). Hypercapnia abolished the oscillation in brain NADH (52). The same group found that hypercapnia did not affect the NADH oxidation level induced by electrical stimulation of the cortex (92, 128, 129). The effects of P_{CO_2} were tested in other organs apart from the brain. Sonn et al. (227) found that dog hypopnea, which induced hypercapnia, changed the redox state of NADH depending on the heart rate.

Exposure of intact animals to CO mimics human CO intoxication requiring an optimal therapeutic strategy (241). Dora et al. (68) were able to change the NADH redox state when CO was applied topically to the brain. Our group showed in detail the influence of various CO levels on the pathophysiology of the brain in vivo (173, 186, 188, 212). When CO levels were low, the NADH remained the same; whereas >3,000 ppm, CO led to an increase in NADH due to the development of hypoxia. In all these studies, we correlated the changes in NADH to other physiological parameters monitored from the same brain area. The negative effects of CO on brain NADH responses to cortical spreading depression were reversed by exposing the rats to hyperbaric oxygenation (212).

Responses to energy consumption changes

As shown by Chance and Williams (57, 58), the activation of the mitochondria by increased ADP is coupled with oxidation of NADH (decreased NADH levels) and is known as the state 4 to state 3 transition in isolated mitochondria. Most of the investigations in this field of tissue activation were made on neuronal tissue in vivo. However, studies of other organs, such as the heart or skeletal muscle, were conducted as well. The demand for energy (ATP) by various tissues is dependent on the specific tasks of each organ or tissue. Nevertheless, the stimulation of mitochondrial function is common in all tissues in the body. We will describe the effects of tissue activation on NADH fluorescence under normoxic conditions as well as during limitation of O_2 supply in the tissue (hypoxia, ischemia).

Brain activation. DIRECT CORTICAL STIMULATION. Direct cortical stimulation of the cerebral tissue is the less drastic event affecting the energy requirement of the tissue, compared with epileptic activity or cortical spreading depression. Rosenthal and Jobsis correlated the effects of direct cortical stimulation on the fluorescence of the intact cerebral cortex (213). A small but significant oxidation of NADH was recorded depending on the stimulation parameters. The same results were obtained when trains of stimuli were applied to the hippocampus of cats (140). A coupling between extra cellular K^+ and the decrease in NADH fluorescence has been documented. This type of study has been later repeated by other investigators who found the same basic pattern of responses. Namely, in the normoxic brain, NADH became oxidized under stimulation (128–130, 139, 141, 143, 226). LaManna et al. (135) found that intensive direct cortical stimulation of the hypoxic cerebral cortex resulted in NADH elevation instead of the typical oxidation (decrease).

BRAIN ACTIVATION BY EPILEPTIC ACTIVITY. The first detailed report on the influence of epileptiform activity on brain cerebral cortex mitochondrial NADH redox state was published by Jobsis et al. in 1971 (110). With the use of anesthetized cats exposed to an epileptogenic drug (Metrazol or Strychnine), a marked expected oxidation of NADH was recorded. Synchronization of the electrical activity increased the demand for energy to restore ionic homeostasis disturbed by epileptic activity. They had proven that brain hypoxia or anoxia did not develop during the epileptic activity and was not the reason for the termination of bursting. A year later, the same group found similar responses under exposure of cat hippocampus to penicillin (191). During seizures, the decrease in NADH was due to its oxidation and not because of a decrease in NAD^+ reduction. The connection between the concentration of K^+ and the decrease in mitochondrial NADH was shown in cat hippocampus (192). The effect of seizures on mitochondrial NADH was investigated later on by other groups, mainly in cat models (66, 69, 100, 131, 143, 220, 226, 236, 253, 254). Vern et al. (253) showed that epileptic activity, induced in hypotensive cats, caused an increase in NADH instead of a decrease.

In 1975, we published our first paper on mitochondrial responses to epileptic activity measured in nonanesthetized rats (159). A clear oxidation of NADH was found, even when Metrazol was applied epidurally. Under hypoxia induction (by 10%, 7.5%, and 5% O_2), the typical oxidation of NADH during epileptic activity took place, but the curve shape was modified. In most of our studies, we found that the response to epileptic activity was followed by a wave of cortical spreading depression (CSD) (148, 150, 152). We found a similar coupling of NADH oxidation with CSD development, when epileptic activity was developed due to O_2 toxicity induced by exposing the rat to hyperbaric oxygenation (151, 153, 167, 177).

Figure 10 presents the progression of seizure activity in a special strain of gerbils, developing epileptic effects as a result of monotonic noise or other factors (168). As seen, the exposure of the awake gerbil to noise resulted in the development of epileptic activity followed by a CSD wave. The coupling between the two pathological events is clear, and manifested by the electrical activity (ECoG) as well as extracellular K^+ levels and NADH redox state. During the epileptic stage, extra cellular potassium increased and started to recover to the baseline, but then a larger elevation was recorded. There is a clear correlation between the various parameters during epilepsy and CSD. The decrease in NADH was smaller during the first stage, followed by an oxidation cycle typical for CSD.

RESPONSES TO CSD. Since the discovery of brain CSD by Leao in 1944, it has become clear that the wave of depolarization passing through the tissue increases energy consumption (138). The effects of CSD on brain mitochondrial NADH was first described in 1973, and a clear oxidation wave was recorded (157, 215). A year later, we demonstrated the coupling between the elevated extracellular K^+ induced by CSD and the greater ATP requirement (NADH oxidation) needed to recover the normal ionic homeostasis (184). This coupling suggests that upon stimulation of Na^+-K^+-ATPase, the released ADP will be recovered by the mitochondria to ATP. This stimulation of the respiratory chain will increase O_2 consumption and, consequently, blood flow will be increased to compensate for the extra O_2 needed (181). Extra O_2 supply or compensation can be achieved by either an increase of CBF, enhanced O_2 extraction, or both. In a well-controlled study, we showed that concomitantly to NADH oxidation and extracellular K^+ changes, CBF doubled while O_2 extraction ratio remained the same (181).

Since our group has published the majority of papers dealing with mitochondrial NADH and CSD, we will start the discussion by describing papers published by others. One of the leading groups, headed by Frans Jobsis, published several studies showing the effects of CSD on brain energy metabolism (135, 136, 143, 215, 226, 234). Several works have been published by Chance and collaborators (96, 97), in addition to those done in collaboration with Mayevsky. Dora's group published two papers in this field (69, 129). Rosenthal and Martel (214) showed that ischemia affected the response to CSD, namely, instead of NADH oxidation, an increase in NADH was recorded (see also Fig. 9, *B* and *C*). Recently, Hashimoto et al. (98) used fluorescence imaging to characterize NADH changes in CSD.

Our group has published over 30 papers (see Table 1) on the relationship between mitochondrial NADH redox state and CSD. Also, we reported, for the first time, the development of CSD in the brain of a comatose patient (162): the details will be discussed further on. Typical responses to CSD monitored in the brain of an awake rat are shown in Fig. 9. In Fig. 9*A*, it is possible to see the correlation between the depression of electrical activity (ECoG) and the oxidation (decrease) of NADH, in triplicate. Figure 9, *B* and *C*, shows a comparison between the responses to CSD in a normoxic and partially ischemic brain. As it can be seen, the typical "oxidation cycle" of NADH was replaced in the ischemic brain by a "reduction cycle" due to a decrease in O_2 compensation capabilities. This interrelation between the responses to cortical spreading depression and the metabolic state of the brain has been studied in detail by our group (see Table 1).

Activation of body organs. The effects of tissue activity on mitochondrial NADH were investigated in the late 1950s. As shown in Fig. 6, the addition of ADP to resting isolated mitochondria (state 4) may lead to an increase in O_2 consumption and oxidation of NADH.

In 1959 Chance and Jobsis (41) applied the newly developed NADH fluorometric method to frog sartorius muscle in vitro and found a decrease in NADH due to a series of twitches leading to an increased ATP breakdown into ADP. Chance

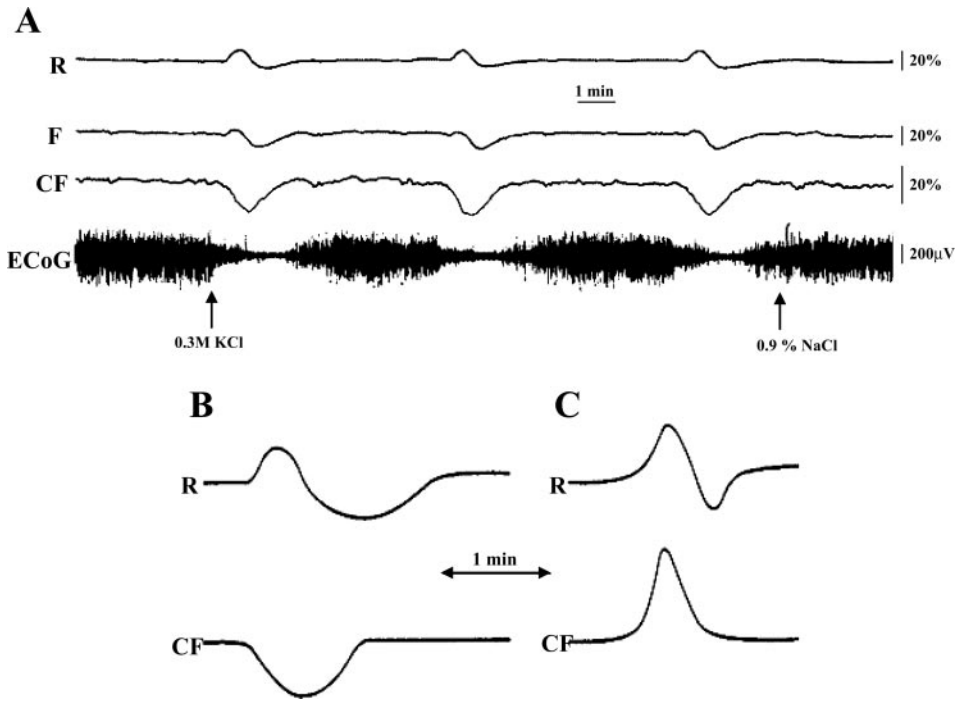

Fig. 9. The development of epileptic activity followed by cortical spreading depression (CSD) in the brain of a seizure-prone gerbil. ECoG, electrocorticogram; Po_2, partial pressure of O_2 in the tissue; $E_K{}^+$, $DC_K{}^+$, extracellular potassium and DC steady potential measured around the K^+ electrode; R, F, and CF, reflectance, NADH fluorescence, and corrected NADH fluorescence.

(28) applied the same approach to monitor the toad sartorius muscle in vivo and found a clear NADH oxidation depending on the rate of stimulation. Systemic injection of epinephrine into the stimulated muscle induced an increase in NADH. Subjecting the highly stimulated muscle to partial hypoxia, induced a further increase in NADH redox state. Chance's studies of the muscle and NADH were summarized in 1966 (31).

A few years ago, Pal et al. (199) monitored NADH fluorescence in cats subjected to sympathetic trunk stimulation. They found that high stimulation frequency caused a large decrease in capillary blood volume and an increase in NADH levels.

As shown in *Brain activation*, activation of the brain by either one of the three methods, leads to oxidation of NADH due to the state 4 to state 3 transition of the mitochondria. The prerequisite for such responses is a normal blood flow that has the capacity to increase O_2 supply to cope with an increased demand.

Activation of the heart may lead to the development of a more complicated situation, since the blood supply will be affected by changes in the muscle contractility. Using dog heart in vivo, Kedem et al. (114) showed that an increase in the heart rate above 150 beats/min leads to an increase in NADH levels, even when the blood flow is enhanced. These results indicated that the autoregulation of blood flow was insufficient to compensate for the extra O_2 needed. The same group tested the effect of inotropic agents on the NADH level in the dog heart in vivo (1). A marked oxidation of NADH was recorded after infusion of norepinephrine or ouabain, concomitantly with the developed increase in

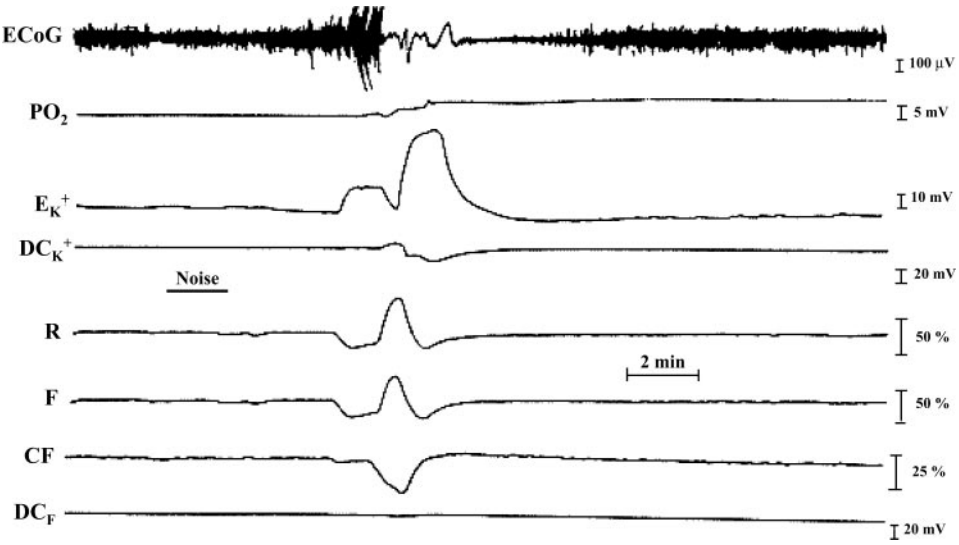

Fig. 10. Responses to CSD induced by 0.3 M KCl applied epidurally in the awake rat. In *A*, the stimulus was maintained on the brain and therefore repeated cycles were recorded. *B* and *C* schematize the responses to CSD recorded in the normoxic and partially ischemic cerebral cortex.

tension. The same group published several more studies, in which they monitored NADH in the heart exposed to other physiological and pathophysiological conditions (2, 76). When the heart rate was elevated from 150 to 280 beats/min, the NADH was elevated but the relative levels of NADH were significantly lower after hypopnea (227) or after injection of nitroprusside (76).

Under ischemia induction (230), the NADH became elevated and the local contractile force decreased compared with the simultaneously measured nonischemic region in the left ventricle. An increase in the heart rate in this model, attenuated the typical increase in blood flow and NADH in the nonischemic region. In the ischemic area, a very small reaction was recorded, indicating that some responsiveness to inotropic simulation was retained.

Effects of pharmacological agents. The effects of various agents on mitochondrial NADH were studied in different organs also under in vivo conditions. Naturally, the in vivo brain was targeted by the most pharmacological agents. The effects of anesthesia or other respiratory chain inhibitors were mainly studied in vitro; however, in vivo experiments were conducted as well. In a pioneering work in 1962, Chance et al. (36) succeeded in showing the different responses of the brain and kidney to Amytal and norepinephrine. Because of inhibition of Site I by Amytal injection, the brain and the kidney showed a clear increase in NADH. After injection of norepnephrine, the brain NADH became oxidized while the kidney NADH was elevated to the level of anoxia. In 1967, Chance showed that in the activated brain (stimulated by Metrazol), the addition of Amytal blocked the epileptic activity and NADH increased in a dose-dependent manner (32). Dora and collaborators (71) significantly contributed to these studies. They tested the influence of phenoxybenzamine on the blood volume and NADH in hypotensive and hypertensive cats. Later on, Dora et al. (72) studied the effects of topical administration of norepinephrine and acetylcholine on blood volume and NADH in the cats' brains. The effects of the adrenergic β-blocker on NADH and blood volume were reported (73). The effects of adenosine (127) and other drugs were described by the same group (67). Rex et al. (208) reported on pharmacological manipulations of brain NADH. The effects of other drugs on NADH were studied by Urbanics et al. (249), Vern et al. (255), and Anderson and Meyer (6). Our group published many papers describing the action of various drugs, including anesthetics, on brain NADH in various brain models (176, 182, 258).

The effects of pharmacological agents on NADH redox state in various organs were published as well. Kedem et al. researched the influence of various inotropic agents (1) as well as nitroprusside (2), nitroglycerin (76), and propranolol (86).

Osbakken and collaborators (194, 195) also monitored NADH under various drug exposures. Baron et al. (17) described the effects of lidocaine on NADH, during ischemia in the dog heart. The effects of blood substitute emulsion on NADH in the kidney were reported (260). The influence of radioprotective chemicals on NADH in rat tissue was described in the 1960s (103). The action of various drugs (e.g., the uncoupler Amytal) was studied in the liver exposed to hyperbaric oxygenation (31, 40).

MONITORING HUMAN BODY ORGANS

The first attempt to apply NADH fluorometry to human tissues in vivo was made in 1971 by Jobsis et al. (111). Using NADH fluorescence microfluorometry, they monitored the exposed brain of neurosurgical patients undergoing treatments for focal cerebral seizures. They correlated the electrocorticographic data to the NADH redox state under direct cortical stimulation of the monitored area. The clear decrease in the NADH signal was interpreted as a change in oxidation. The recorded changes were very similar to those obtained in analogous procedures in the cat brain (213). A few years later, the collaboration between Austin and Chance (8) led to the recording of NADH in the brain of patients subjected to microanastomosis of the superficial temporal artery to the middle cerebral artery. The same group found an improvement of cerebral oxidative metabolism after the anastomosis, which was correlated to the elevated blood flow and increased tissue P_{O_2} (9).

The next step was taken by Barlow et al. (16), who expanded this technique to monitor the heart and the brain. Using a different type of fluorometer, Van Buren et al. showed a decrease in NADH (oxidation) due to cortical stimulation in epileptic patients (251). In 1979, Fein and Jobsis (81) studied the changes in brain energetics in patients undergoing superficial temporal arterial-middle cerebral artery microanastomosis. Fein and Olinger (82, 83) monitored patients after transient ischemic attacks. The brain of these patients, who had undergone an extracranial-intracranial bypass, was stimulated, and changes in NADH were recorded.

The laser-based fluorimeter developed by Renault (207) was used to monitor NADH redox state in the heart muscle during pharmacological treatments (207), as well as in skeletal muscle (91). Attempts to apply NADH fluorometry in clinical practice (reported in a dozen short publications) did not lead to the development of a proper medical device applicable on a daily basis.

In 1990, our team started developing a unique multiparametric monitoring system that included the measurement of NADH fluorescence, using a light guide-based device. This system was initially applied to monitor neurosurgical patients undergoing brain surgery or those treated in the intensive care unit. In the first paper on the subject (published in 1991), we showed the feasibility of our approach. After a transient short occlusion of one common carotid artery, the increase in NADH was correlated to a decrease in cerebral blood flow (164). It took another 5 years to restart organized clinical testing of our monitoring system. In the second half of the 1990s (162, 172), we were able to monitor the brain of comatose patients in the intensive care unit and describe the development of spreading depression-like responses, including marked NADH reactions. A modified multiparametric monitoring system was applied for NADH measurement during neurosurgical procedures in the operating room (173). Later on, we attempted to apply our monitoring system to human kidney during a transplantation procedure. We measured the transplanted kidney cortex immediately after the surgical procedures (178). An apparent oxidation of NADH, immediately after reopening the renal artery, was correlated to an increase in microcirculatory blood flow.

Recordings from a head-injured patient (Fig. 11, *A* and *B*) demonstrate the importance of the multiparametric monitoring approach. The responses to spreading depression SD (Fig. 11*A*)

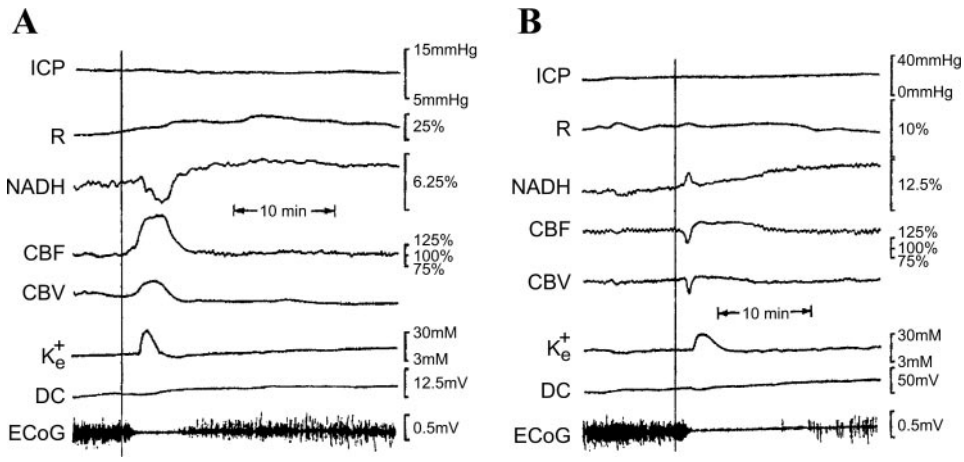

Fig. 11. Two responses of the brain (*A*, *B*) to a wave of CSD developed spontaneously in a severely head-injured patient. ICP, intracranial pressure; R, NADH, 366 nm reflectance and 450 nm corrected fluorescence; CBF, CBV, cerebral blood flow and volume measured by laser Doppler flowmetry; K^+, DC, extracellular potassium levels and the DC steady potential measured around the K^+ electrode.

were typical for the first five SD cycles, recorded 4.5 h after the beginning of the monitoring period. The responses shown in Fig. 11*B*, however, were typical for repetitive 35–40 cycles developed every 20–30 min later on in the same patient.

In the SD cycle shown in Fig. 11*A*, the depolarization was characterized by a depression of the ECoG, a large increase in extracellular K^+, and a small negative shift in the DC steady potential. The concomitant hemodynamic and metabolic responses are shown in the oxidation of mitochondrial NADH (decreased NADH) and a large increase in cerebral blood flow (CBF). The depolarization, which developed a few hours later (Fig. 11*B*), appears to be very similar in terms of ECoG, extracellular K^+, and DC potential. The metabolic and hemodynamic responses to this SD cycle are markedly different. The CBF shows a clear biphasic response starting with an initial decrease followed by a small hyperemic response. The same response was recorded by the volume parameter of the laser Doppler flowmeter. The mitochondrial NADH became more reduced (increased) during the hypoperfusion phase. It can be seen from the two figures, that the slower recovery of the ECoG and extracellular K^+ in the second SD, corresponds to the nature of the metabolic and hemodynamic responses.

The observations of human spreading depression using the multiparametric approach (85) and the various responses to it suggest that the basic mechanisms of brain pathophysiological processes may be similar in both the animal and human brain. It is well documented that during the SD wave, which basically involves a propagation of depolarization through the entire hemisphere, a large increase in O_2 consumption occurs due to the stimulation of the ion pumps (88). This increased O_2 demand is compensated by a large increase in cerebral blood flow.

When SD is induced under relatively normal conditions, there is a complete coupling between the increase in O_2 consumption and the large increase in CBF (Fig. 11*A*). On the other hand, under limited O_2 supply (in ischemia or hypoxia), the responses of the brain to SD are altered. The combination of the NADH probe with the CBF probe revealed that the reversed NADH response (an increase instead of a decrease) is due to a limited CBF compensation as indicated by the initial decreased CBF response (Fig. 11*B*). Such important information may help initiate appropriate intervention procedures to avoid additional deterioration. In the past 10 years, we have attempted to develop a commercial device that could be applied in daily medical practice. In 1999, the first tissue spectroscope was developed and received US Food and Drug Administration clearance in 2000. The device enabled the monitoring of NADH fluorescence and tissue reflectance, in combination with a laser Doppler flowmeter for tissue blood flow measurements. This device was tested in neurosurgical patients in the operating room. The details of the device were published in a few articles (see, for example, Ref. 170). In the past 2 years, an upgraded device has been developed to include another parameter in addition to the original three parameters of the tissue spectroscope. This new device, named the CritiView, could be used to monitor any tissue in the body (155).

MONITORING NADH AND THE MULTIPARAMETRIC APPROACH

The need for multiparametric monitoring of other parameters, additional to NADH, results from the basic understanding that NADH is affected by two major factors. The redox state of NADH reflects not only the availability of O_2 inside the mitochondria but also the turnover rate of the ATP-ADP cycling activity (state 4 to state 3 transition). The interaction between these two factors affects the nature of NADH response to various conditions. For example, an increase in energy consumption (e.g., cortical spreading depression) under O_2 restriction will be manifested as an increase in NADH rather than a decrease (oxidation) measured in normal well-oxygenated tissue. According to Chance and Williams, an increase in ATP production is always recorded as a decrease in NADH (57, 58). Therefore, the "reduction cycle" measured by the NADH signal in response to CSD can be interpreted as an artifact of some kind. This phenomenon and the fact that the mitochondrial NADH signal cannot yet be calibrated in absolute values prompted us to develop a multiparametric monitoring approach and a probe that could be used in various tissues exposed to different pathophysiological conditions. By this approach, two major advantages were gained. First, it provided the possibility of a better interpretation of the recorded results; second, nonphysiological responses could also be more easily detected. To elaborate on these points, we will consider the following typical example. In the early stage of NADH monitoring using a time sharing fluorometer, we found that a few minutes after complete ischemia was induced by decapitation in a rat model, a large increase in the reflectance signal was

recorded in parallel to a clear NADH decrease in the dead monitored brain, apparently indicative of NADH oxidation. We termed this event "the Secondary Reflectance Increase-SRI" (147). It was clear to us that this late "oxidation" of NADH in the dead animal was an artifact of the monitoring system. The same response was recorded also when partial ischemia was induced in a gerbil's brain. The "oxidation" of NADH in a dead or partially ischemic brain did not have any physiological or biochemical interpretation, so we suspected that this "oxidation" is due to the large increase in the reflectance signal, and to a failure of the fluorescence signal's correction method. We speculated that the large increase in the reflectance trace (SRI) after ischemia or brain death, resulted from a spasm of blood vessels. Such spasms are known to occur in this type of conditions, namely during cortex depolarization. Only when monitoring other parameters, in addition to NADH, such as extracellular K+ and DC steady potential, were we able to give a substantial explanation for the SRI event (85). On the basis of these experiments, we concluded that the SRI phenomenon is always associated with a negative shift in the DC potential and a large increase in extracellular potassium when energy is not available.

In subsequent studies, when we added the monitoring of CBF (laser Doppler flowmetry) to the multiparametric system, we became able to complete the explanation of the SRI event (164). A partial ischemia model in the gerbil revealed that after the initial decrease in blood flow and increase in NADH, the secondary recorded event was very similar to SRI. During the SRI, CBF decreased to very low levels and NADH was further elevated, at the same time as the DC potential and extracellular K^+ accumulated as typical for a depolarization event. We concluded that under various pathological brain conditions, depolarization may lead to severe vasoconstriction (decrease in blood volume) due to the accumulated potassium. In this case, an artifact will be recorded in NADH measurements due to the SRI. This detailed example illustrates the advantages of monitoring other physiological parameters in addition to NADH fluorescence. In the next few sections, we will present, in chronological order, the various parameters that have been added to NADH measurements. In all these studies, NADH is the most important parameter, while the inclusion of other parameters improves our ability to explain pathophysiological processes.

NADH and electrical activity

The first attempt to combine NADH and electrical measurements was made by Chance and Schoener in 1962 (50). They showed the time relationship between the increase in NADH due to anoxia or hypoxia, and the disappearance of electrical activity (ECoG) in rat cerebral cortex. The same type of correlation was reported later by Jobsis et al. (110) for epileptic activity, and by Rosenthal and Somjen (163) and Mayevsky and Chance (157) for CSD. The accumulated results have made it clear that under limited energy or O_2 supply, NADH becomes elevated in the brain, while the spontaneous ECoG activity is depressed. The ECoG begins to decelerate when NADH reaches 70%-80% of its maximal increase upon death (157, 159) or decapitation (160, 259). The recovery of ECoG after anoxia is completed much later than NADH oxidation, suggesting that energy availability is a prerequisite condition but not the only condition needed for a complete ECoG recovery. Depression of the ECoG is also recorded when the brain is exposed to depolarization due to CSD; however, it is not caused by a lack of O_2. Similar correlations between NADH and ECoG were described in cat cerebral cortex exposed to seizures and hemorrhagic hypotension (100).

NADH, ECoG, DC potential, and extracellular K^+

In 1974, we correlated the responses of NADH to CSD, with changes in ECoG, extracellular K^+ (measured by microelectrodes) and DC steady potential (184). Similar results were published a year later by Lothman et al. (143) and subsequently by other investigators (references not cited).

NADH and respiratory chain components

Since the activities of various respiratory chain components are strongly coupled, the tissue respiratory rate can be better evaluated by monitoring several such components. Very few attempts have been made to correlate NADH responses in vivo, with other components of the respiratory chain. The main reason for this was the stronger interference of blood with Fp

Table 2. *Historical milestones in monitoring NADH fluorescence in vivo*

Year	Discovery/Activity	Authors
1957	The first detailed study using NADH fluorescence spectrophotometry	Duysens and Amesz (75)
1958	Measurements of NADH fluorescence in isolated mitochondria	Chance and Baltscheffsky (34)
1959	Testing the effect of stimulation on NADH fluorescence in excised frog sartorious muscle	Chance and Jöbsis (41)
1962	In vivo monitoring of NADH fluorescence in brain and kidney	Chance et al. (36)
1965	Comparison between NADH fluorescence in vivo and enzymatic analysis of tissue NADH	Chance et al. (39)
1968	Monitoring tissue reflectance in addition to NADH fluorescence	Jöbsis and Stansby (112)
1971	The first attempt to monitor the human brain during a neurosurgical procedure	Jöbsis et al. (111)
1973	The first fiber optic based fluorometer-reflectometer used in the brain of an awake animal	Chance et al. (48); Mayevsky and Chance (157)
1982	Simultaneous monitoring of NADH in vivo in four different organs in the body	Mayevsky and Chance (161)
1985	Monitoring of brain NADH together with ^{31}P NMR Spectroscopy	Mayevsky et al. (180)
1991	Simultaneous real time monitoring of NADH, CBF, ECoG, and extracellular ions in experimental animals and in the neurosurgical operating room	Mayevsky et al. (164)
1996	The multiparametric response (including NADH) to cortical spreading depression is for the first time measured in a comatose patient	Mayevsky et al. (162)
2000	Development of the FDA-approved "tissue spectroscope" medical device for real-time monitoring of NADH and tissue blood flow	Mayevsky et al. (170)
2006	Monitoring of tissue vitality (NADH, TBF, and HbO_2) by a new "CritiView" device	Mayevsky et al. (155)

FDA, food and drug administration; CBF, cerebral blood flow; ECoG, electrocorticogram; TBF, taste bud fragment.

or cytochrome oxidase measurements, compared with NADH. The effects of hypotension and anoxia on NADH and cytochrome aa3, were measured in the brain in vivo (99). LaManna et al. showed the effects of Ethanol on brain NADH and cytochrome aa3 in rats and cats (137). Therefore, almost all correlations between Fp and NADH were studied in blood-free organs (49). In 1976, we presented preliminary results indicating that in certain morphological areas of the brain, containing less blood vessels, a good correlation is recorded between NADH and Fp responses to anoxia in vivo (146). The only practical way to measure these two signals together was to freeze the tissue and then analyze the two parameters in the frozen state (168, 183). Another approach to correlating NADH and Fp redox state was suggested by Paddle et al. (198). They used a NADH/Fp scanning fluorometer to monitor the muscle (198) or rat diaphragm (197). A few papers have been published on the use of flying spot fluorometer to monitor the two fluorescent signals in the brain and other organs (35). Most of the data published in this field have been acquired in vitro (33, 49) or in blood-free organs such as the liver (218).

Monitoring NADH, ionic, hemodynamic, and electrical activities

The multiparametric monitoring approach was expanded by Dora et al. (74) by the addition of the Po_2 parameter to NADH, reflectance, extracellular K^+, DC steady potential, and ECoG. We showed in the gerbil brain that anesthesia affected the NADH, Po_2, and ECoG (169).

To improve the multiparametric probe, it was necessary to include the various sensors in a single holder that could be used on a daily basis without too many technical difficulties. In the new probe, all sensors touched the brain surface (after removal of the dura mater without penetration into the tissue itself) (169). Using the same principles, we were able to develop a new generation of multiprobe assemblies that have been used in our laboratory during the past 25 years (Figs. 10 and 11). Here, several relevant publications are cited (85, 150–152, 166). The next significant step was the embedding of a laser Doppler flowmeter sensor into the multiprobe assembly to monitor the continuous microcirculatory blood flow, in addition to NADH, Reflectance, extracellular K^+ and Ca^{2+}, and ECoG and DC potential (164). In 1996, we included in the multiprobe assembly a sensor to monitor intracranial pressure (ICP). This device was applied to human brain (162) and rat models (14).

The in vivo multiparametric monitoring approach has been also applied to other organs in the body. Kedem's group supplemented NADH measurements of dog heart, with the monitoring of tissue blood flow by heat clearance and of isometric contractile tension (2). Our group used the multiparametric monitoring system to study the function of rat kidney in vivo (3). The influence of ischemia on NADH and microcirculatory blood flow was studied in rat liver in vivo (15). The correlation between NADH and other parameters, such as microcirculatory blood flow and/or ^{31}P-NMR, was monitored in the beating heart in vivo (194) and in the brain in vivo (180). Presently, due to technological developments, it is possible to integrate the monitoring of NADH with any other type of monitoring systems, either in animal studies or various clinical applications. As mentioned earlier, a unique multiparametric monitoring system based on light-emitting diodes and laser diodes, is available (155). The system is connected to the tissue by a flexible bundle of excitation and emission fibers, and provides real time information on NADH redox state, microcirculatory blood flow, tissue reflectance and HbO_2.

SUMMARY AND CONCLUSIONS

In this review, we tried to summarize the scientific background and technological aspects of in vivo NADH fluometry approach for the monitoring of mitochondrial functions. This technology still has some limitations including the need for better correction technique for hemodynamic artefacts as well as a new approach for quantitative calibration of the signals. During the past decade, the preliminary application of the NADH fluorometry to clinical environment was very promising. This stimulates us to improve the technology to provide a practical medical device that will be used by many clinicians after approval by the regulatory agencies around the world.

REFERENCES

1. **Acad B, Guggenheimer E, Sonn J, Kedem J.** Differential effects of various inotropic agents on the intracellular NADH redox level in the in vivo dog heart. *J Cardiovasc Pharmacol* 5: 284–290, 1983.
2. **Acad B, Sonn J, Furman E, Scheinowitz M, Kedem J.** Specific effects of nitroprusside on myocardial O_2 balance following coronary ligation in the dog heart. *J Cardiovasc Pharmacol* 9: 79–86, 1987.
3. **Amran-Cohen D, Sonn J, Luger-Hamer M, Mayevsky A.** The effect of ischemia and hypoxia on renal blood flow, energy metabolism and function in vivo. *Adv Exp Med Biol* 540: 93–101, 2003.
4. **Anderson-Engels S, Wilson BC.** In vivo fluorescence in clinical oncology: fundamental and practical issues. *J Cell Pharmacol* 3: 66–79, 1992.
5. **Anderson RE.** Instrumentation for in vivo cerebral NADH studies in squirrel monkey. *IEEE Trans Biomed Eng* BME-22: 220–224, 1975.
6. **Anderson RE, Meyer FB.** Nitric oxide synthase inhibition by L-NAME during repetitive focal cerebral ischemia in rabbits. *Am J Physiol Heart Circ Physiol* 271: H588–H594, 1996.
7. **Aubert X, Chance B, Keynes RD.** Optical studies of biochemical events in the electric organ of *Electrophorus*. *Proc R Soc Lond B Biol Sci* 160: 211–245, 1964.
8. **Austin G, Jutzy R, Chance B, Barlow C.** Noninvasive monitoring of human brain oxidative metabolism. *Adv Exp Med Biol* III: 1445–1455, 1978.
9. **Austin G, Jutzy R, Hill W, Chance B, Barlow C.** Cortical oxidative metabolism: a measure of collateral flow in microanastomoses. In: *Proceedings of the World Microsurgical Congress*, San Francisco, CA, 1978.
10. **Avi-Dor Y, Olson JM, Doherty MD, Kaplan NO.** Fluorescence of pyridine nucleotides in mitochondria. *J Biol Chem* 237: 2377–2383, 1962.
11. **Avontuur JAM, Ashruff J, Uzermans JNM, Scheringa M, Ince C, Bruining HA.** NADH videofluorimetry reveals early gut ischemia caused by tumor necrosis factor. *Pflügers Arch* 418: R141–R1521991. (Abstract).
12. **Balaban RS, Mandel LJ.** Coupling of aerobic metabolism to active ion transport in the kidney. *J Physiol* 304: 331–348, 1980.
13. **Balaban RS, Mandel LJ.** Metabolic substrate utilization by rabbit proximal tubule. An NADH fluorescence study. *Am J Physiol Renal Fluid Electrolyte Physiol* 254: F407–F416, 1988.
14. **Barbiro-Micahely E, Mayevsky A.** Multiparametric monitoring of brain under elevated intracranial pressure in a rat model. *J Neurotrauma* 18: 711–725, 2001.
15. **Barbiro E, Zurovsky Y, Mayevsky A.** Real time monitoring of rat liver energy state during ischemia. *Microvasc Res* 56: 253–260, 1998.
16. **Barlow CH, Harden WR, III, Harken AH, Simson MB, Haselgrove JC, Chance B, O'Connor M, Austin G.** Fluorescence mapping of mitochondrial redox changes in heart and brain. *Crit Care Med* 7: 402–406, 1979.
17. **Baron DW, Walls JT, Anderson RE, Harrison CE Jr.** Protective effect of lidocaine during regional myocardial ischemia. *Mayo Clin Proc* 57: 442–447, 1982.

18. **Bickler PE, Koh SO, Severinghaus JW.** Effects of hypoxia and hypocapnia on brain redox balance in ducks. *Am J Physiol Regul Integr Comp Physiol* 257: R132–R135, 1989.
19. **Boldt M, Harbig K, Weidemann G, Lubbers DW.** A sensitive dual wavelength microspectrophotometer for the measurement of tissue fluorescence and reflectance. *Pflügers Arch* 385: 167–173, 1980.
20. **Bradley RS, Thorniley MS.** A review of attenuation correction techniques for tissue fluorescence. *J Royal Soc Int* 3: 1–13, 2006.
21. **Brandes R, Figueredo VM, Camacho SA, Massie BM, Weiner MW.** Suppression of motion artifacts in fluorescence spectroscopy of perfused hearts. *Am J Physiol Heart Circ Physiol* 263: H972–H980, 1992.
22. **Brandes R, Maier LS, Bers DM.** Regulation of mitochondrial [NADH] by cytosolic [Ca^{2+}] and work in trabeculae from hypertrophic and normal rat hearts. *Circ Res* 82: 1189–1198, 1998.
23. **Brauser B, Bucher T, Dolivo M.** Redox transitions of cytochromes and pyridine nucleotides upon stimulation of an isolated rat ganglion. *FEBS Lett* 8: 297–300, 1970.
24. **Bruining HA, Pierik GJM, Ince C, Ashruf F.** Optical spectroscopic imaging for non-invasive evaluation of tissue oxygenation. *Chirurgie* 118: 317–323, 1992.
25. **Chance B.** Spectra and reaction kinetics of respiratory pigments of homogenized and intact cells. *Nature* 169: 215–221, 1952.
26. **Chance B.** Enzyme mechanisms in living cells. In: *The Mechanism of Enzyme Action*, edited by McElroy WD and Glass B. Baltimore, MD: Johns Hopkins Press, 1954, p. 399–453.
27. **Chance B.** Spectrophotometry of intracellular respiratory pigments. *Science* 120: 767–775, 1954.
28. **Chance B.** Continuous recording of intracellular reduced pyridine nucleotide changes in skeletal muscle in vivo. *Tex Rep Biol Med* 22: 836–841, 1964.
29. **Chance B.** Reaction of oxygen with the respiratory chain in cells and tissues. *J Gen Physiol* 49: 163–188, 1965.
30. **Chance B.** The energy-linked reaction of calcium with mitochondria. *J Biol Chem* 240: 2729–2748, 1965.
31. **Chance B.** The identification and control of metabolic states. *Genootschap ter Bevordering van Natuur-, Genees-, en Heelkunde te Amsterdam* 5–37, 1966.
32. **Chance B.** Biochemical studies of transitions from rest to activity. In: *Sleep and Altered States of Consciousness* (vol. XLV). Baltimore, MD: Williams & Wilkins, 1967, p. 48–63.
33. **Chance B.** The kinetics of flavoprotein and pyridine nucleotide oxidation in cardiac mitochondria in the presence of calcium. *FEBS Lett* 26: 315–319, 1972.
34. **Chance B, Baltscheffsky H.** Respiratory enzymes in oxidative phosphorylation. VII. Binding of intramitochondrial reduced pyridine nucleotide. *J Biol Chem* 233: 736–739, 1958.
35. **Chance B, Barlow C, Nakase Y, Takeda H, Mayevsky A, Fischetti R, Graham N, Sorge J.** Heterogeneity of oxygen delivery in normoxic and hypoxic states: a fluorometer study. *Am J Physiol Heart Circ Physiol* 235: H809–H820, 1978.
36. **Chance B, Cohen P, Jobsis F, Schoener B.** Intracellular oxidation-reduction states in vivo. *Science* 137: 499–508, 1962.
37. **Chance B, Conrad H, Legallias V.** Simultaneous fluorimetric and spectrophotometric measurements of reaction kinetics of bound pyridine nucleotide in mitochondria (Abstract). *Biophysical Soc Meet* 441958, year?.
38. **Chance B, Graham N, Mayer D.** A time sharing fluorometer for the readout of intracellular oxidation-reduction states of NADH and flavoprotein. *Rev Sci Instrum* 42: 951–957, 1971.
39. **Chance B, Jamieson D, Coles H.** Energy-linked pyridine nucleotide reduction: inhibitory effects of hyperbaric oxygen in vitro and in vivo. *Nature* 4981: 257–263, 1965.
40. **Chance B, Jamieson D, Williamson JR.** Control of the oxidation-reduction state of reduced pyridine nucleotides in vivo and in vitro by hyperbaric oxygen. *Third International Conference on Hyperbaric Medicine, National Academy of Sciences*, city?, 15–41, 1966.
41. **Chance B, Jobsis F.** Changes in fluorescence in a frog sartorius muscle following a twitch. *Nature* 184: 195–196, 1959.
42. **Chance B, Legallias V.** Differential microfluorimeter for the localization of reduced pyridine nucleotide in living cells. *Rev Sci Instrum* 30: 732–735, 1959.
43. **Chance B, Legallias V, Schoener B.** Metabolically linked changes in fluorescence emission spectra of cortex of rat brain, kidney and adrenal gland. *Nature* 195: 1073–1075, 1962.
44. **Chance B, Legallias V, Schoener B.** Combined fluorometer and double-beam spectrophotometer for reflectance measurements. *Rev Sci Instrum* 34: 1307–1311, 1963.
45. **Chance B, Legallias V, Sorge J, Graham N.** A versatile time-sharing multichannel spectrophotometer reflectometer and fluorometer. *Anal Biochem* 66: 498–514, 1975.
46. **Chance B, Lieberman M.** Intrinsic fluorescence emission from the cornea at low temperatures: Evidence of mitochondrial signals and their differing redox states in epithelial and endothelial sides. *Exp Eye Res* 26: 111–117, 1978.
47. **Chance B, Mayevsky A, Goodwin C, Mela L.** Factors in oxygen delivery to tissue. *Microvasc Res* 8: 276–282, 1974.
48. **Chance B, Oshino N, Sugano T, Mayevsky A.** Basic principles of tissue oxygen determination from mitochondrial signals. In: *Int Symposium on Oxygen Transport to Tissue, Adv Exp Med Biol* (vol. 37A), Bicher HI and Bruley DF (Eds.). New York: Plenum, 1973, p. 277–292.
49. **Chance B, Salkovitz IA, Kovach AGB.** Kinetics of mitochondrial flavoprotein and pyridine nucleotide in perfused heart. *Am J Physiol* 223: 207–218, 1972.
50. **Chance B, Schoener B.** Correlation of oxidation-reduction changes of intracellular reduced pyridine nucleotide and changes in electro-encephalogram of the rat in anoxia. *Nature* 195: 956–958, 1962.
51. **Chance B, Schoener B, Krejci K, Russmann W, Wesemann W, Schnitger H, Bucher T.** Kinetics of fluorescence and metabolite changes in rat liver during a cycle of ischemia. *Biochemische Zeitschrift* 341: 325–333, 1965.
52. **Chance B, Schoener B, Oshino R, Itshak F, Nakase Y.** Oxidation-reduction ratio studies of mitochondria in freeze-trapped samples. NADH and flavoprotein fluorescence signals. *J Biol Chem* 254: 4764–4771, 1979.
53. **Chance B, Schoener B, Schindler F.** The intracellular oxidation-reduction state. In: *Oxygen in the Animal Organism*, edited by Dickens F and Neil E. London, Pergamon, 1963, p. 367–392.
54. **Chance B, Thorell B.** Fluorescence measurements of mitochondrial pyridine nucleotide in aerobiosis and anaerobiosis. *Nature* 184: 931–934, 1959.
55. **Chance B, Thorell B.** Localization and kinetics of reduced pyridine nucleotide in living cells by microfluorometry. *J Biol Chem* 234: 3044–3050, 1959.
56. **Chance B, Williams GR.** A method for the localization of sites for oxidative phosphorylation. *Nature* 176: 250–254, 1955.
57. **Chance B, Williams GR.** Respiratory enzymes in oxidative phosphorylation (III-The steady state). *J Biol Chem* 217: 409–427, 1955.
58. **Chance B, Williams GR.** The respiratory chain and oxidative phosphorylation. In: *Advances in Enzymology* (vol. 17), edited by Nord FF. New York: Interscience, 1956, p. 65–134.
59. **Chance B, Williamson JR, Jamieson D, Schoener B.** Properties and kinetics of reduced pyridine nucleotide fluorescence of the isolated and in vivo rat heart. *Biochemische Zeitschrift* 341: 357–377, 1965.
60. **Chapman JB.** Fluorometric studies of oxidative metabolism in isolated papillary muscle of the rabbit. *J Gen Physiol* 59: 135–154, 1972.
61. **Connelly CM, Chance B.** Kinetics of reduced pyridine nucleotides in stimulated frog muscle and nerve (Abstract). *American Physiological Society* 13: 29, 1954.
62. **Cordeiro PG, Kirschner RE, Hu QY, Chiao JJC, Savage H, Alfano RR, Hoffman LA, Hidalgo DA.** Ultraviolet excitation fluorescence spectroscopy: A noninvasive method for the measurement of redox changes in ischemic myocutaneous flaps. *Plast Reconstr Surg* 96: 673–680, 1995.
63. **Coremans JMCC, Ince C, Bruining HA, Puppels GJ.** (Semi-)quantitative analysis of reduced nicotinamide adenine dinucleotide fluorescence images of blood-perfused rat heart. *Biophys J* 72: 1849–1860, 1997.
64. **Coremans JMCC, Van Aken M, Naus DC, Van Velthuysen ML, Bruining HA, Puppels GJ.** Pretransplantation assessment of renal viability with NADH fluorimetry. *Kidney Int* 57: 671–683, 2000.
65. **Doane MG.** Fluorometric measurement of pyridine nucleotide reduction in the giant axon of the squid. *J Gen Physiol* 50: 2603–2632, 1967.
66. **Dora E.** Glycolysis and epilepsy-induced changes in cerebrocortical NAD/NADH redox state. *J Neurochem* 41: 1774–1777, 1983.
67. **Dora E.** Further studies on reflectometric monitoring of cerebrocortical microcirculation. Importance of lactate anions in coupling between cerebral blood flow and metabolism. *Acta Physiol Hung* 66: 199–211, 1985.

68. **Dora E, Chance B, Kovach AGB, Silver IA.** Carbon monoxide-induced localized toxic anoxia in the rat brain cortex. *J Appl Physiol* 39: 875–878, 1975.
69. **Dora E, Gyulai L, Kovach AGB.** Determinants of brain activation-induced cortical NAD/NADH responses in vivo. *Brain Res* 299: 61–72, 1984.
70. **Dora E, Kovach AGB.** Factors influencing the correction factor used to eliminate the apparent NADH fluorescence changes caused by alterations in cerebrocortical blood content. *Adv Exp Med Biol* 94: 113–118, 1978.
71. **Dora E, Kovach AGB.** Effect of acute arterial hypo- and hypertension on cerebrocortical NAD/NADH redox state and vascular volume. *J CBF Metab* 2: 209–219, 1982.
72. **Dora E, Kovach AGB.** Effect of topically administered epinephrine, norepinephrine, and acetylcholine on cerebrocortical circulation and the NAD/NADH redox state. *J CBF Metab* 3: 161–169, 1983.
73. **Dora E, Kovach AGB.** Effect of the adrenergic beta receptor blocker propranolol on the dilatation of cerebrocortical vessels evoked by arterial hypoxia. *Acta Physiol Hung* 63: 35–41, 1984.
74. **Dora E, Zeuthen T, Silver IA, Kovach AGB.** Effect of arterial hypoxia on the cerebrocortical redox state, vascular volume, oxygen tension, electrical activity and potassium ion concentration. *Acta Physiol Acad Sci Hung* 54: 319–331, 1979.
75. **Duysens LNM, Amesz J.** Fluorescence spectrophotometry of reduced phosphopyridine nucleotide in intact cells in the near-ultraviolet and visible region. *Biochim Biophys Acta* 24: 19–26, 1957.
76. **Dvir S, Acad BA, Sonn J, Furman E, Kedem J.** Preservation of myocardial oxygen balance and functional reserve by coronary vasodilators. *Arch Int Physiol Biochim Biophys* 93: 231–239, 1985.
77. **Dzeja PP, Holmuhamedov EL, Ozcan C, Pucar D, Jahangir A, Terzic A.** Mitochondria: gateway for cytoprotection. *Circ Res* 89: 744–746, 2001.
78. **Eng J, Lynch RM, Balaban RS.** Nicotinamide adenine dinucleotide fluorescence spectroscopy and imaging of isolated cardiac myocytes. *Biophys J* 55: 621–630, 1989.
79. **Ernster L, Schatz G.** Mitochondria: a historical review. *J Cell Biol* 91: 227s-255s, 1981.
80. **Estabrook RW.** Fluorometric measurement of reduced pyridine nucleotide in cellular and subcellular particles. *Anal Biochem* 4: 231–245, 1962.
81. **Fein J, Jobsis F.** Brain energetics in patients undergoing STA-MCA microanastomosis. *Acta Neurol Scand Suppl* 72: 504–505, 1979.
82. **Fein JM.** NADH kinetics in patients with unruptured aneurysms versus cerebrovascular occlusive disease. *J CBF Metab* 3: S29–S30, 1983.
83. **Fein JM, Olinger R.** Cortical nicotinamide adenine dinucleotide (NADH) kinetics in patients undergoing extracranial-intracranial bypass. *Neurosurgery* 10: 428–436, 1982.
84. **Franke H, Barlow CH, Chance B.** Oxygen delivery in perfused rat kidney: NADH fluorescence and renal functional state. *Am J Physiol* 231: 1082–1089, 1976.
85. **Friedli CM, Sclarsky DS, Mayevsky A.** Multiprobe monitoring of ionic,metabolic, and electrical actiities in the awake brain. *Am J Physiol Regul Integr Comp Physiol* 243: R462–R469, 1982.
86. **Furman E, Acad BA, Sonn J, Raul A, Kedem J.** Effect of global vs. regional ischaemia upon myocardial contractility and oxygen balance. *Cardiovasc Res* 19: 606–612, 1985.
87. **Galeotti T, van Rossum GDV, Mayer DH, Chance B.** On the fluorescence of NAD(P)H in whole-cell preparations of tumours and normal tissues. *Eur J Biochem* 17: 485–496, 1970.
88. **Gloor P.** Migrane and regional cerebral blood flow. *Trends Neurosci* 9: 21, 1986.
89. **Gosalvez M, Thurman RG, Chance B, Reinhold H.** Mammary tumours in vivo demonstrated by fluorescence of pyridine nucleotide. *Br J Radiol* 45: 510–514, 1972.
90. **Granholm L, Lukjanova L, Siesjo BK.** Tissue NADH levels in the rat brain during pronounced hyperventilation. *Acta Physiol Scand* 72: 533–534, 1968.
91. **Guezennec CY, Lienhard F, Louisy F, Renault G, Tusseau MH, Portero P.** In situ NADH laser fluorimetry during muscle contraction in humans. *Eur J Appl Physiol* 63: 36–42, 1991.
92. **Gyulai L, Dora E, Kovach AGB.** NAD/NADH: redox state changes on cat brain cortex during stimulation and hypercapnia. *Am J Physiol Heart Circ Physiol* 243: H619–H627, 1982.
93. **Harbig K, Chance B, Kovach AGB, Reivich M.** In vivo measurement of pyridine nucleotide fluorescence from cat brain cortex. *J Appl Physiol* 41: 480–488, 1976.
94. **Harden A, Young W.** Alcoholic ferment of yeast-juice. Part II. Co-ferment of yeast-juice. *Proc R Soc Lond B Biol Sci* B78: 369–375, 1906.
95. **Harrison M, Sick TJ, Rosenthal M.** Mitochondrial redox responses to cerebral ischaemia produced by four-vessel occlusion in the rat. *Neurol Res* 7: 142–148, 1985.
96. **Haselgrove J, Barlow C, Eleff E, Chance B, Lebordais S.** Correlation of electrical signals and mitochondrial redox state during spreading depression. In: *Oxygen Transport to Tissue* (vol. 25), edited by Kovach AGB, Dora E, Kessler M, and Silver IA. Budapest, Hungary: Pergamon, 1981, p. 25–26.
97. **Haselgrove J, Barlow CH, Chance B.** The 3D distribution of metabolic states in the gerbil brain during the course of spreading depression. In: *Cerebral Metabolism and Neural Function*, edited by Passoneau JV, Hawkins RA, Lust WD, and Welsh FA. Baltimore/London: Williams & Wilkins, 1980, p. 72–76.
98. **Hashimoto M, Takeda Y, Sato T, Kawahara H, Nagano O, Hirakawa M.** Dynamic changes of NADH fluorescence images and NADH content during spreading depression in the cerebral cortex of gerbils. *Brain Res* 872: 294–300, 2000.
99. **Hempel FG, Jobsis FF.** Comparison of cerebral NADH and cytochrome AA_3 redox shifts during anoxia or hemorrhagic hypotension. *Life Sci* 25: 1145–1152, 1979.
100. **Hempel FG, Kariman K, Saltzman HA.** Redox transitions in mitochondria of cat cerebral cortex with seizures and hemorrhagic hypotension. *Am J Physiol Heart Circ Physiol* 238: H249–H256, 1980.
101. **Horvath KA, Torchiana DF, Daggett WM, Nishioka NS.** Monitoring myocardial reperfusion injury with NADH fluorometry. *Lasers Surg Med* 12: 2–6, 1992.
102. **Ince C, Coremans JMCC, Bruining HA.** In vivo NADH fluorescence. In: *Adv Exp Med: Oxygen Transport to Tissue XIV*, edited by Erdmann W and Bruley DF. New York: Plenum, 1992, p. 277–296.
103. **Jamieson D, Van den Brenk HA.** Studies of mechanisms of chemical radiation protection in vivo. III. Changes in fluorescence of intracellular pyridine nucleotides and modification by extracellular hypoxia. *Int J Radiat Biol* 10: 223–241, 1966.
104. **Ji S, Chance B, Nishiki K, Smith T, Rich T.** Micro-light guides: a new method for measuring tissue fluorescence and reflectance. *Am J Physiol Cell Physiol* 236: C144–C156, 1979.
105. **Ji S, Lemasters JJ, Christenson V, Thurman RG.** Periportal and pericentral pyridine nucleotide fluorescence from the surface of the perfused liver: evaluation of the hypothesis that chronic treatment with ethanol produces pericentral hypoxia. *Proc Natl Acad Sci USA* 79: 5415–5419, 1982.
106. **Jobsis FF.** Intracellular metabolism of oxygen. *Am Rev Respir Dis* 110: 58–63, 1974.
107. **Jobsis F, Legallias V, O'Connor M.** A regulated differential fluorometer for the assay of oxidative metabolism in intact tissues. *IEEE Trans Biomed Eng* BME-13: 93–99, 1966.
108. **Jobsis FF, Duffield JC.** Oxidative and glycolytic recovery metabolism in muscle. Fluorometric observations on their relative contributions. *J Gen Physiol* 50: 1009–1047, 1967.
109. **Jobsis FF, LaManna JC.** Kinetic aspects of intracellular redox reactions. In vivo effects during and after hypoxia and ischemia. In: *Extrapulmonary Manifestations of Respiratory Disease*, edited by Robin E. New York: Dekker, 1978, p. 63–106.
110. **Jobsis FF, O'Connor M, Vitale A, Vreman H.** Intracellular redox changes in functioning cerebral cortex. I. Metabolic effects of epileptiform activity. *J Neurophysiol* 3465: 735–749, 1971.
111. **Jobsis FF, O'Connor MJ, Rosenthal M, Van Buren JM.** Fluorometric monitoring of metabolic activity in the intact cerebral cortex. In: *Neurophysiology Studied in Man. Proceeding of a Symposium*, edited by Somjen GG. Paris, 20–22, Excerpta Medica International Congress Series, no. 253, 1971, p. 18–26.
112. **Jobsis FF, Stainsby WN.** Oxidation of NADH during contractions of circulated mammalian skeletal muscle. *Respir Physiol* 4: 292–300, 1968.
113. **Kaminogo M.** The effects of mild hyperoxia and/or hypertension on oxygen availability and oxidative metabolism in acute focal ischaemia. *Neurol Res* 11: 145–149, 1989.
114. **Kedem J, Mayevsky A, Sonn J, Acad B.** An experimental approach for evaluation of the O_2 balance in local myocardial regions in vivo. *Q J Exp Physiol* 66: 501–514, 1981.

115. **Kedem J, Sonn J, Scheinowitz M, Weiss HR.** Relationship between local oxygen consumption and local and external cardiac work: effect of tachycardia. *Cardiovasc Res* 23: 1043–1052, 1989.
116. **Kelly JJ, Rorvik DA, Richmond KN, Barlow CH.** Videofluoremeter for imaging tissue metabolism. *Rev Sci Instrum* 60: 3498–3502, 1989.
117. **Kessler M, Hoper J, Chance B, Lubbers DW, Messmer K, Sinagowitz E.** Regulation of reactive hyperaemia in the kidney. In: *Oxygen Transport to Tissue VII*, edited by Kreuzer F, Cain SM, Turek Z, and Goldstick TK. New York and London: Plenum, 1985, p. 683–692.
118. **Kessler M, Hoper J, Lubbers DW, Ji S.** Local factors affecting regulation of microflow, O_2 uptake and energy metabolism. In: *Oxygen Transport to Tissue*, edited by Kovach AGB, Dora E, Kessler M, and Silver IA. City: Publisher, 1981, p. 155–162.
119. **Kitai T, Tanaka A, Tokuka A, Ozawa K, Iwata S, Chance B.** Changes in the redox distribution of rat liver by ischemia. *Anal Biochem* 206: 131–136, 1992.
120. **Klingenberg M, Slenczka W, Ritt E.** Vergleichende biochemie der pyridinnucleotid-systeme in mitochondrien verschiedener organe. *Biochem Z* 332: 47–66, 1959.
121. **Kobayashi S, Kaede K, Nishiki K, Ogata E.** Microfluorometry of oxidation-reduction state of the rat kidney in situ. *J Appl Physiol* 31: 693–696, 1971.
122. **Kobayashi S, Nishiki K, Kaede K, Ogata E.** Optical consequences of blood substitution on tissue oxidation- reduction state microfluorometry. *J Appl Physiol* 31: 93–96, 1971.
123. **Kohen E, Kohen C, Thorell B.** Use of microfluorimetry to study the metabolism of intact cells. *Biomed Eng* 00: 554–565, 1969.
124. **Kohen E, Kohen C, Thorell B, Schachtschabel D.** Multisite analysis of metabolic transients in single living cells by multichannel microfluorometry. *Mikrochim Acta* 1: 223–236, 1975.
125. **Koretsky AP, Balaban RS.** Changes in pyridine nucleotide levels alter oxygen consumption and extra-mitochondrial phosphates in isolated mitochondria: a ^{31}P-NMR and NAD(P)H fluorescence study. *Biochim Biophys Acta* 893: 398–408, 1987.
126. **Koretsky AP, Katz LA, Balaban RS.** Determination of pyridine nucleotide fluorescence from the perfused heart using an internal standard. *Am J Physiol Heart Circ Physiol* 253: H856–H862, 1987.
127. **Kovach AGB, Dora E.** Contribution of adenosine to the regulation of cerebral blood flow: the role of calcium ions in the adenosine-induced cerebrocortical vasodilatation. *Adv Exp Med Biol* 169: 315–325, 1984.
128. **Kovach AGB, Dora E, Gyulai L.** Effects of microcirculation on microfluorometric measurements. In: *Oxygen and Physiological Function*, edited by Jobsis FF. Dallas: Professional Information Library, 1977, p. 111–123.
129. **Kovach AGB, Dora E, Gyulai L.** Relationship between steady redox state and brain activation-induced NAD/NADH redox responses. *Adv Exp Med Biol* 169: 81–100, 1984.
130. **Kovach AGB, Dora E, Gyulai L, Eke A.** Cerebrovascular and metabolic reactions at the CBF autoregulatory level evoked by electrical stimulation of the cat brain cortex. *Basel* 15: p. 371–374, 1977.
131. **Kovach AGB, Dora E, Szedlacsek S, Koller A.** Effect of the organic calcium antagonist D-600 on cerebrocortical vascular and redox responses evoked by adenosine, anoxia and epilepsy. *J CBF Metab* 3: 51–61, 1983.
132. **Kramer RS, Pearlstein RD.** Cerebral cortical microfluorometry at isosbestic wavelengths for correction of vascular artifact. *Science* 205: 693–696, 1979.
133. **Kraut A, Barbiro-Michaely E, Mayevsky A.** Differential effects of norepinephrine on brain and other less vital organs detected by a multisite multiparametric monitoring system. *Med Sci Monit* 10: BR215-BR220, 2004.
134. **LaManna J.** In vivo *control of oxidative metabolism monitored in intact cerebral cortex by optical techniques* (PhD thesis). Durham, NC: Department of Physiology and Pharmacology, Duke University, 1975 pp., 1991.
135. **LaManna JC, Peretsman SJ, Light AI, Rosenthal M.** Oxygen sufficiency in the "working" brain. In: *Oxygen Transport to Tissue*, edited by Kovach AGB, Dora E, and Silver IA. 1981, p. 95–96.
136. **LaManna JC, Rosenthal M.** Effect of ouabain and phenobarbital on oxidative metabolic activity associated with spreading cortical depression in cats. *Brain Res* 88: 145–149, 1975.
137. **LaManna JC, Younts BW Jr, Rosenthal M.** The cerebral oxidative metabolic response to acute ethanol administration in rats and cats. *Neuropharmacology* 16: 283–288, 1977.
138. **Leao AAP.** Spreading depression of activity in cerebral cortex. *J Neurophysiol* 7: 359–390, 1944.
139. **Leniger-Follert E, Urbanics R, Harbig K, Lubbers DW.** The behavior of local pH and NADH-fluorescence during and after direct activation of the brain cortex. In: *Cerebral Function Metabolism and Circulation* (vol. 56), edited by Ingvar DH and Lassen NA. Copenhagen, Denmark: Acta Neurologica Scandinavica, 1977, p. 214–215.
140. **Lewis DV, Schuette WH.** NADH fluorescence and $[K^+]_o$ changes during hippocampal electrical stimulation. *J Neurophysiol* 38: 405–417, 1975.
141. **Lewis DV, Schuette WH.** NADH fluorescence $[K^+]_o$ and oxygen consumption in cat cerebral cortex during direct cortical stimulation. *Brain Res* 110: 523–535, 1976.
142. **Lipton P.** Effects of membrane depolarization on nicotinamide nucleotide fluorescence in brain slices. *Biochem J* 136: 999–1009, 1973.
143. **Lothman E, LaManna J, Cordingley G, Rosenthal M, Somjen G.** Responses of electrical potential potassium levels, and oxidative metabolic activity of the cerebral neocortex of cats. *Brain Res* 88: 15–36, 1975.
144. **Lowry OH, Passonneau JV, Hasselberger FX, Schulz DW.** Effect of ischemia on known substrates and cofactors of the glycolytic pathway in brain. *J Biol Chem* 239: 18–30, 1964.
145. **Mandel LJ, Riddle TG, LaManna JC.** A rapid scanning spectrophotometer and fluorometer for in vivo monitoring of steady state and kinetic optical properties of respiratory enzymes. In: *Oxygen and Physiological Function*, edited by Jobsis FF. Dallas, TX: Profession Information Library, 1976, p. 79–89.
146. **Mayevsky A.** Brain energy metabolism of the conscious rat exposed to various physiological and pathological situations. *Brain Res* 113: 327–338, 1976.
147. **Mayevsky A.** Ischemia in the brain: The effects of carotid artery ligation and decapitation on the energy state of the awake and anesthetized rat. *Brain Res* 140: 217–230, 1978.
148. **Mayevsky A.** Shedding light on the awake brain. In: *Frontiers in Bienergetics: From Electrons to Tissues* (vol. 2), edited by Dutton PL, Leigh J, and Scarpa A. New York: Academic, 1978, p. 1467–1476.
149. **Mayevsky A.** The responses of an awake brain to HPO under increased CO_2 concentration. In: *Oxygen Transport to Tissue III*, edited by Silver IA, Erecinska M, and Bicher HI. New York: Plenum, 1978, p. 735–740.
150. **Mayevsky A.** Metabolic, ionic and electrical responses to experimental epilepsy in the awake rat. In: *Proc First International Congress of Cerebral Blood Flow, Metabolism & Epilepsy*, edited by Baldy M, Moulinier DH, Ingvar DH, and Meldrum BS, and John Libbey. city?: publisher?, 1983, p. 263–270.
151. **Mayevsky A.** Multiparameter monitoring of the awake brain under hyperbaric oxygenation. *J Appl Physiol* 54: 740–748, 1983.
152. **Mayevsky A.** Brain NADH redox state monitored in vivo by fiber optic surface fluorometry. *Brain Res Rev* 7: 49–68, 1984.
153. **Mayevsky A.** Brain oxygen toxicity. In: *Underwater Physiology*, edited by Bachrach AJ and Matzen MM. Bethesda, MD: Undersea Medical Society, 1984, p. 69–89.
154. **Mayevsky A.** Level of ischemia and brain functions in the Mongolian gerbil in vivo. *Brain Res* 524: 1–9, 1990.
155. **Mayevsky A, Blum Y, Dekel N, Deutsch A, Halfon R, Kremer S, Pewzner E, Sherman E, Barnea O.** The CritiView–A new fiber optic based optical device for the assessment of tissue vitality. *Proc SPIE* 6083: 60830Z-1–60830Z-9, 2006.
156. **Mayevsky A, Breuer Z.** Brain vasculature and mitochondrial responses to ischemia in gerbils. I. Basic anatomical patterns and biochemical correlates. *Brain Res* 58: 242–250, 1992.
157. **Mayevsky A, Chance B.** A new long-term method for the measurement of NADH fluorescence in intact rat brain with implanted cannula. In: *Oxygen Transport to Tissue, Adv Exp Med Biol* (vol. 37A), edited by Bicher HI and Bruley DF. New York: Plenum, 1973, p. 239–244.
158. **Mayevsky A, Chance B.** Repetitive patterns of metabolic changes during cortical spreading depression of the awake rat. *Brain Res* 65: 529–533, 1974.
159. **Mayevsky A, Chance B.** Metabolic responses of the awake cerebral cortex to anoxia hypoxia spreading depression and epileptiform activity. *Brain Res* 98: 149–165, 1975.
160. **Mayevsky A, Chance B.** The effect of decapitation on the oxidation-reduction state of NADH and ECoG in the brain of the awake rat. II. Oxygen transport to tissue. *Adv Exp Med Biol* 75: 307–312, 1976.

161. **Mayevsky A, Chance B.** Intracellular oxidation reduction state measured in situ by a multichannel fiber-optic surface fluorometer. *Science* 217: 537–540, 1982.
162. **Mayevsky A, Doron A, Manor T, Meilin S, Zarchin N, Ouaknine GE.** Cortical spreading depression recorded from the human brain using a multiparametric monitoring system. *Brain Res* 740: 268–274, 1996.
163. **Mayevsky A, Duckrow RB, Yoles E, Zarchin N, Kanshansky D.** Brain mitochondrial redox state, tissue hemodynamic and extracellular ion responses to four-vessel occlusion and spreading depression in the rat. *Neurol Res* 12: 243–248, 1990.
164. **Mayevsky A, Flamm ES, Pennie W, Chance B.** A fiber optic based multiprobes system for intraoperative monitoring of brain functions. *SPIE* 1431: 303–313, 1991.
165. **Mayevsky A, Frank K, Muck M, Nioka S, Kessler M, Chance B.** Multiparametric evaluation of brain functions in the Mongolian gerbil in vivo. *J Basic Clin Physiol Pharmacol* 3: 323–342, 1992.
166. **Mayevsky A, Friedli CM, Reivich M.** Metabolic, ionic and electrical responses of the gerbil brain to ischemia. *Am J Physiol Regul Integr Comp Physiol* 248: R99–R107, 1985.
167. **Mayevsky A, Jamieson D, Chance B.** Oxygen poisoning in the unanesthetized brain: correlation of the oxidation-reduction state of pyridine nucleotide with electrical activity. *Brain Res* 76: 481–491, 1974.
168. **Mayevsky A, Kaplan H, Haveri J, Haselgrove J, Chance B.** Three-dimensional metabolic mapping of the freeze-trapped brain: Effects of ischemia on the Mongolian gerbil. *Brain Res* 367: 63–72, 1986.
169. **Mayevsky A, Lebourdais S, Chance B.** The interrelation between brain PO_2 and NADH oxidation-reduction state in the gerbil. *J Neurosci Res* 5: 173–182, 1980.
170. **Mayevsky A, Manor T, Pevzner E, Deutsch A, Etziony R, Dekel N.** Real-time optical monitoring of tissue vitality in vivo. *Proc SPIE* 4616: 30–39, 2002.
171. **Mayevsky A, Manor T, Pevzner E, Deutsch A, Etziony R, Dekel N, Jaronkin A.** Tissue spectroscope: a novel in vivo approach to real time monitoring of tissue vitality. *J Biomed Opt* 9: 1028–1045, 2004.
172. **Mayevsky A, Meilin S, Manor T, Ornstein E, Zarchin N, Sonn J.** Multiparametric monitoring of brain oxygen balance under experimental and clinical conditions. *Neurol Res* 20: S76–S80, 1998.
173. **Mayevsky A, Meilin S, Rogatsky GG, Zarchin N, Sonn J.** Multiparametric monitoring of the awake brain exposed to carbon monoxide. *J Appl Physiol* 78: 1188–1196, 1995.
174. **Mayevsky A, Mizawa I, Sloviter HA.** Surface fluorometry and electrical activity of the isolated rat brain perfused with artificial blood. *Neurol Res* 3: 307–316, 1981.
175. **Mayevsky A, Nakache R, Luger-Hamer M, Amran D, Sonn J.** Assessment of transplanted kidney vitality by a multiparametric monitoring system. *Transplant Proc* 33: 2933–2934, 2001.
176. **Mayevsky A, Rogatsky GG, Sonn J.** New multiparametric monitoring approach for real-time evaluation of drug tissue interaction in vivo. *Drug Dev Res* 50: 457–470, 2000.
177. **Mayevsky A, Shaya B.** Factors affecting the development of hyperbaric oxygen toxicity in the awake rat brain. *J Appl Physiol* 49: 700–707, 1980.
178. **Mayevsky A, Sonn J, Luger-Hamer M, Nakache R.** Real time assessment of organ vitality during the transplantation procedure. *Transplantation Rev* 17: 96–116, 2003.
179. **Mayevsky A, Subramanian VH, Chance B.** Brain oxidative metabolism of the newborn dog: Correlation between ^{31}P NMR spectroscopy and pyridine nucleotides redox state. *J CBF Metab* 8: 201–207, 1988.
180. **Mayevsky A, Subramanian VH, Nioka S, Barlow C, Haselgrove J, Chance B.** Brain energy metabolism evaluated simultaneously in the newborn dog by ^{31}P NMR spectroscopy and NADH fluorometry/reflectometry in vivo. *J CBF Metab Suppl*: 400–401, 1985.
181. **Mayevsky A, Weiss HR.** Cerebral blood flow and oxygen consumption in cortical spreading depression. *J CBF Metab* 11: 829–836, 1991.
182. **Mayevsky A, Zarchin N, Friedli CM.** Factors affecting the oxygen balance in the awake cerebral cortex exposed to spreading depression. *Brain Res* 236: 93–105, 1982.
183. **Mayevsky A, Zarchin N, Kaplan H, Haveri J, Haselgrove J, Chance B.** Brain metabolic responses to ischemia in the Mongolian gerbil: in vivo and freeze trapped redox state scanning. *Brain Res* 276: 95–107, 1983.
184. **Mayevsky A, Zeuthen T, Chance B.** Measurements of extracellular potassium, ECoG and pyridine nucleotide levels during cortical spreading depression in rats. *Brain Res* 76: 347–349, 1974.
185. **Mayevsky A, Ziv I.** Oscillations of cortical oxidative metabolism and microcirculation in the ischemic brain. *Neurol Res* 13: 39–47, 1991.
186. **Meilin S, Sonn J, Zarchin N, Rogatsky G, Guggenheimer-Furman E, Mayevsky A.** Responses of rat brain to induced spreading depression following exposure to carbon monoxide. *Brain Res* 780: 323–328, 1998.
187. **Meilin S, Zarchin N, Mayevsky A.** Inter-relation between hemodynamic, metabolic, ionic and electrical activities during ischemia and reperfusion in the gerbil brain. *Neurol Res* 21: 699–704, 1999.
188. **Mendelman A, Zarchin N, Meilin S, Guggenheimer-Furman E, Thom SR, Mayevsky A.** Blood flow and ionic responses in the awake brain due to carbon monoxide. *Neurol Res* 24: 765–772, 2002.
189. **Mills SA, Jobsis FF, Seaber AV.** A fluorometric study of oxidative metabolism in the in vivo canine heart during acute ischemia and hypoxia. *Ann Surg* 186: 193–200, 1977.
190. **Nuutinen EM.** Subcellular origin of the surface fluorescence of reduced nicotinamide nucleotides in the isolated perfused rat heart. *Basic Res Cardiol* 79: 49–58, 1984.
191. **O'Connor MJ, Herman CJ, Rosenthal M, Jobsis F.** Intracellular redox changes preceding onset of epileptiform activity in intact cat hippocampus. *J Neurophysiol* 35: 471–483, 1972.
192. **O'Connor MJ, Lewis DV, Herman CJ.** Effects of potassium on oxidative metabolism and seizures. *Electroencephalogr Clin Neurophysiol* 35: 205–208, 1973.
193. **O'Connor MJ, Welsh F, Komarnicky L, Davis L, Stevens J, Lewis D, Herman C.** Origin of labile NADH tissue fluorescence. *Oxygen Physiol Function* 00: 90–99, 1977.
194. **Osbakken M, Blum H, Wang DJ, Doliba N, Ivanics T, Zhang D, Mayevsky A.** In vivo mechanisms of myocardial functional stability during physiological interventions. *Gen Cardiol* 79: 1–13, 1991.
195. **Osbakken M, Doliba N, Mitchell MD, Ivanics T, Zhang D, Mayevsky A.** Acetylcholine: Is it a myocardial metabolic regulator? *J Appl Cardiol* 5: 357–366, 1990.
196. **Osbakken M, Mayevsky A.** Multiparameter monitoring and analysis of in vivo ischemic and hypoxic heart. *J Basic Clin Physiol Pharmacol* 7: 97–113, 1996.
197. **Paddle BM.** A cytoplasmic component of pyridine nucleotide fluorescence in rat diaphragm: evidence from comparisons with flavoprotein fluorescence. *Pflügers Arch* 404: 326–331, 1985.
198. **Paddle BM, Brown G, Vincent P.** Scanning fluorometer for the rapid assessment of pyridine nucleotide and flavoprotein fluorescence changes in tissues in vivo. *J Biomed Eng* 8: 334–340, 1986.
199. **Pal M, Toth A, Ping P, Johnson PC.** Capillary blood flow and tissue metabolism in skeletal muscle during sympathetic trunk stimulation. *Am J Physiol Heart Circ Physiol* 274: H430–H440, 1998.
200. **Perez-Pinzon MA, Mumford PL, Rosenthal M, Sick TJ.** Antioxidants, mitochondrial hyperoxidation and elecrical recovery after anoxia in hippocampal slices. *Brain Res* 754: 163–170, 1997.
201. **Perry RP, Thorell B, Akerman L, Chance B.** Localization and assay of respiratory enzymes in single living cells. Absorbency measurements on the Nebenkern. *Nature* 184: 929–931, 1959.
202. **Pfeifer L, Paul R, Yalcin E, Marx U, Konig F, Fink F.** A time-gated laser spectrometer using optical fibres for detecting fluorescent biomolecules in cells and tissue. In: *Monitoring Molecules in Neuroscience*, edited by Gonzalez-Mora JL, Borges R, and Mas M. Santa Cruz de Tenerife, Spain: University of La Laguna, 1996, p. 42–43.
203. **Pierik EGJM, Ince C, Avontuur JAM, Ashruff J, Bruining HA.** The application of NADH fluorescence to identify noninvasively tissue hypoxia in vivo. *Eur Surg Res* 23: 12–13, 1991.
204. **Rahmer H, Kessler M.** Influence of hemoglobin concentration in perfusate and in blood on fluorescence of pyridine nucleotides (NADH and NADPH) of rat liver. In: *Adv Exp Med Biol: Oxygen Transport to Tissue*, edited by Bicher HI and Bruley DF. New York: Plenum press, 1973, p. 377–382.
205. **Rampil IJ, Litt L, Mayevsky A.** Correlated, simultaneous, multiple-wavelength optical monitoring in vivo of localized cerebrocortical NADH and brain microvessel hemoglobin oxygen saturation. *J Clin Monit* 8: 216–225, 1992.
206. **Renault G, Raynal E, Cornillault J.** Cancelling of Fresnel reflection in in situ, double beam laser, fluorimetry using a single optical fiber. *J Biomed Eng* 5: 243–247, 1983.
207. **Renault G, Raynal E, Sinet M, Berthier JP, Godard B, Cornillault J.** A laser fluorimeter for direct cardiac metabolism investigation. *Optics Laser Technol* 00: 143–148, 1982.

208. **Rex A, Pfeifer L, Fink F, Fink H.** Cortical NADH during pharmacological manipulations of the respiratory chain and spreading depression in vivo. *J Neurosci Res* 57: 359–370, 1999.
209. **Riess ML, Camara AK, Chen Q, Novalija E, Rhodes SS, Stowe DF.** Altered NADH and improved function by anesthetic and ischemic preconditioning in guinea pig intact hearts. *Am J Physiol Heart Circ Physiol* 283: H53–H60, 2002.
210. **Riess ML, Novalija E, Camara AK, Eells JT, Chen Q, Stowe DF.** Preconditioning with sevoflurane reduces changes in nicotinamide adenine dinucleotide during ischemia-reperfusion in isolated hearts: reversal by 5-hydroxydecanoic acid. *Anesthesiology* 98: 387–395, 2003.
211. **Rink R, Kessler M, Hajek K.** *Signs of Hypoxia in the Small Intestine of the Rat During Hemorrhagic Shock* (vol. 37A). city?: publisher?, 1973, p. 469–475.
212. **Rogatsky GG, Meilin S, Zarchin N, Thom SR, Mayevsky A.** Hyperbaric oxygenation affects rat brain function after carbon monoxide exposure. *Undersea Hyperb Med* 29: 50–58, 2002.
213. **Rosenthal M, Jobsis FF.** Intracellular redox changes in functioning cerebral cortex. II. Effects of direct cortical stimulation. *J Neurophysiol* 34: 750–762, 1971.
214. **Rosenthal M, Martel DL.** Ischemia-induced alterations in oxidative "recovery" metabolism after spreading cortical depression in situ. *Exp Neurol* 63: 367–378, 1979.
215. **Rosenthal M, Somjen G.** Spreading depression, sustained potential shifts, and metabolic activity of cerebral cortex of cats. *J Neurophysiol* 36: 739–749, 1973.
216. **Salama G, Lombardi R, Elson J.** Maps of optical action potentials and NADH fluorescence in intact working hearts. *Am J Physiol Heart Circ Physiol* 252: H384–H394, 1987.
217. **Scheffler IE.** A century of mitochondrial research: achievements and perspectives. *Mitochondrion* 1: 3–31, 2000.
218. **Scholz R, Thurman RG, Williamson JR, Chance B, Bucher T.** Flavin and pyridine nucleotide oxidation-reduction changes in perfused rat liver. *J Biol Chem* 244: 2317–2324, 1969.
219. **Schomacker KT, Frisoli JK, Compton CC, Flotte TJ, Richter JM, Nishioka NS, Deutsch TF.** Ultraviolet laser-induced fluorescence of colonic tissue: basic biology and diagnostic potential. *Lasers Surg Med* 12: 63–78, 1992.
220. **Schuchmann S, Buchheim K, Meierkord H, Heinemann U.** A relative energy failure is associated with low-Mg^{2+} but not with 4-aminopyridine induced seizure-like events in entorhinal cortex. *J Neurophysiol* 81: 399–403, 1999.
221. **Shiino A, Matsuda M, Handa J, Chance B.** Poor recovery of mitochondrial redox state in CA1 after transient forebrain ischemia in gerbils. *Stroke* 29: 2421–2424, 1998.
222. **Shimazaki J, Tornheim K, Laing RA.** Correlation of redox fluorometry and analytical measurements of pyridine nucleotide. *Invest Ophthalmol Vis Sci* 30: 2274–2278, 1989.
223. **Sick TJ, Perez-Pinzon MA.** Optical methods for probing mitochondrial function in brain slices. *Methods* 18: 104–108, 1999.
224. **Simonovich M, Barbiro-Michaely E, Salame K, Mayevsky A.** A new approach to monitor spinal cord vitality in real time. *Adv Exp Med Biol* 540: 125–132, 2003.
225. **Sims NR, Anderson MF.** Mitochondrial contributions to tissue damage in stroke. *Neurochem Int* 40: 511–526, 2002.
226. **Somjen GG, Rosenthal M, Cordingley G, LaManna J, Lothman E.** Potassium, neuroglia, and oxidative metabolism in central gray matter. *Fed Proc* 35: 1266–1271, 1976.
227. **Sonn J, Acad B, Mayevsky A, Kedem J.** Effect of coronary vasodilation produced by hypopnea upon regional myocardial oxygen balance. *Arch Int Physiol Biochim Biophys* 89: 445–455, 1981.
228. **Sonn J, Mayevsky A.** Effects of brain oxygenation on metabolic, hemodynamic, ionic and electrical responses to spreading depression in the rat. *Brain Res* 882: 212–216, 2000.
229. **Sonn J, Mayevsky A.** The effect of ethanol on metabolic, hemodynamic and electrical responses to cortical spreading depression. *Brain Res* 908: 174–186, 2001.
230. **Sonn J, Mayevsky A, Acad B, Guggenheimer E, Kedem J.** Effect of local ischemia on the myocardial oxygen balance and its response to heart rate elevation. *Q J Exp Physiol* 67: 335–348, 1982.
231. **Sundt TM, Anderson RE.** Reduced nicotinamide adenine dinucleotide fluorescence and cortical blood flow in ischemic and nonischemic squirrel monkey cortex. 2. Effects of alterations in arterial carbon dioxide tension, blood pressure, and blood volume. *Stroke* 6: 279–283, 1975.
232. **Sundt TM, Anderson RE.** Reduced nicotinamide adenine dinucleotide fluorescence and cortical blood flow in ischemic and nonischemic squirrel monkey cortex. I. Animal preparation, instrumentation, and validity of model. *Stroke* 6: 270–278, 1975.
233. **Sundt TM Jr, Anderson RE, Sharbrough FW.** Effect of hypocapnia, hypercapnia, and blood pressure on NADH fluorescence, electrical activity, and blood flow in normal and partially ischemic monkey cortex. *J Neurochem* 27: 1125–1133, 1976.
234. **Sylvia AL, Rosenthal M.** Effects of age on brain oxidative metabolism in vivo. *Brain Res* 165: 235–248, 1979.
235. **Takano T, Miyazaki Y, Nashimoto I, Kobayashi K.** Effect of hyperbaric oxygen on cyanide intoxication: in situ changes in intracellular oxidation reduction. *Undersea Biomed Res* 7: 191–197, 1980.
236. **Tenny RT, Sharbrough FW, Anderson RE.** Correlation of intracellular redox states and pH with blood flow in primary and secondary seizure foci. *Ann Neurol* 8: 564–573, 1980.
237. **Terzuolo CA, Chance B, Handelman E, Rossini L, Schmelzer P.** Measurements of reduced pyridine nucleotides in a single neuron. *Biochim Biophys Acta* 126: 361–372, 1966.
238. **Theorell H, Bonnichsen R.** Studies on liver alcohol dehydrogenase. I. Equilibria and initial reaction velocities. *Acta Chem Scand* 5: 1105–1126, 1951.
239. **Theorell H, Chance B.** Studies on liver alcohol dehydrogenase. II. The kinetics of the compound of horse liver alcohol dehydrogenase and reduced diphosphopyridine nucleotide. *Acta Chem Scand* 5: 1127–1144, 1951.
240. **Theorell H, Nygaard AP.** Kinetics and equilibria in flavoprotein systems. I. A fluorescence recorder and its application to a study of the dissociation of the old yellow enzyme and its resynthesis from riboflavin phosphate and protein. *Acta Chem Scand* 8: 877–888, 1954.
241. **Thom SR, Keim LW.** Carbon monoxide poisoning: a review epidemiology, pathophysiology, clinical findings, and treatment options including hyperbaric oxygen therapy. *J Toxicol Clin Toxicol* 27: 141–156, 1989.
242. **Thorniley MS, Lane N, Simpkin S, Fuller B, Jenabzadeh MZ, Green CJ.** Monitoring of mitochondrial NADH levels by surface fluorimetry as an indication of ischaemia during hepatic and renal transplantation. *Adv Exp Med Biol* 388: 431–444, 1996.
243. **Thorniley MS, Simpkin S, Fuller B, Jenabzadeh MZ, Green CJ.** Monitoring of surface mitochondrial NADH levels as an indication of ischemia during liver isograft transplantation. *Hepatology* 21: 1602–1609, 1995.
244. **Thorsrud BA, Harris C.** Real time microfiberoptic redox fluorometry: modulation of the pyridine nucleotide status of the organogenesis-stage rat visceral yolk sac with cyanide and alloxan. *Toxicol Appl Pharmacol* 135: 237–245, 1995.
245. **Thurman RG, Lemasters JJ.** New micro-optical methods to study metabolism in periportal and pericentral regions of the liver lobule. *Drug Metab Rev* 19: 263–281, 1988.
246. **Tomlinson FH, Anderson RE, Meyer FB.** Brain pH_i, cerebral blood flow, and NADH fluorescence during severe incomplete global ischemia in rabbits. *Stroke* 24: 435–443, 1993.
247. **Toth A, Pal M, Tischler ME, Johnson PC.** Are there oxygen-deficient regions in resting skeletal muscle? *Am J Physiol Heart Circ Physiol* 270: H1933–H1939, 1996.
248. **Toth A, Tischler ME, Pal M, Koller A, Johnson PC.** A multipurpose instrument for quantitative intravital microscopy. *J Appl Physiol* 73: 296–306, 1992.
249. **Urbanics R, Greenberg JH, Toffano G, Reivich M.** Effect of GM1 ganglioside after focal cerebral ischemia in halothane-anesthetized cats. *Stroke* 20: 795–802, 1989.
250. **van der Laan L, Coremans A, Ince C, Bruining HA.** NADH videofluorimetry to monitor the energy state of skeletal muscle in vivo. *J Surg Res* 74: 155–160, 1998.
251. **Van Buren JM, Lewis MD, Schuette WH, Whitehouse WC, Marsan CA.** Fluorometric monitoring of NADH levels in cerebral cortex: Preliminary observations in human epilepsy. *Neurosurgery* 2: 114–121, 1978.
252. **Varadarajan SG, An J, Novalija E, Smart SC, Stowe DF.** Changes in $[Na^+]_i$, compartmental $[Ca^{2+}]$, and NADH with dysfunction after global ischemia in intact hearts. *Am J Physiol Heart Circ Physiol* 280: H280–H293, 2001.

253. **Vern B, Schuette WH, Whitehouse WC, Mutsuga N.** Cortical oxygen consumption and NADH fluorescence during metrazol seizures in normotensive and hypotensive cats. *Exp Neurol* 52: 82–99, 1976.
254. **Vern BA, Schuette WH, Mutsuga N, Whitehouse WC.** Effects of ischemia on the removal of extracellular potassium in cat cortex during pentylenetetrazol seizures. *Epilepsia* 20: 711–724, 1979.
255. **Vern BA, Schuette WH, Whitehouse WC.** Effects of brain stem stimulation on cortical NADH fluorescence, blood flow, and O_2 consumption in the cat. *Exp Neurol* 71: 581–600, 1981.
256. **Welsh FA, O'Connor MJ, Langfitt TW.** Regions of cerebral ischemia located by pyridine nucleotide fluorescence (Abstract). *Science* 198: 951–953, 1977.
257. **Wendt IR, Chapman JB.** Fluorometric studies of recovery metabolism of rat fast- and slow-twitch muscles. *Am J Physiol* 230: 1644–1649, 1976.
258. **Zarchin N, Guggenheimer-Furman E, Meilin S, Ornstein E, Mayevsky A.** Thiopental induced cerebral protection during ischemia in gerbils. *Brain Res* 780: 230–236, 1998.
259. **Zarchin N, Mayevsky A.** The effects of age on the metabolic and electrical responses to decapitation in the awake and anesthetized rat brain. *Mech Ageing Dev* 16: 285–294, 1981.
260. **Zurovsky Y, Sonn J.** Fiber optic surface fluorometry-reflectometry technique in the renal physiology of rats. *J Basic Clin Physiol Pharmacol* 3: 343–358, 1992.